Received June 8, 2020, accepted June 20, 2020, date of publication July 13, 2020, date of current version July 23, 2020.

Digital Object Identifier 10.1109/ACCESS.2020.3008778

Probability Based Survey of Braking System: A Pareto-Optimal Approach

AMINREZA KARAMOOZIAN[1], HAOBIN JIANG[1], AND CHIN AN TAN[2]

[1]School of Automotive and Traffic Engineering, Jiangsu University, Zhenjiang 212013, China
[2]Department of Mechanical Engineering, Wayne State University, Detroit, MI 48202, USA

Corresponding author: Aminreza Karamoozian (karamoozian@ujs.edu.cn)

This work was supported in part by the Primary Research and Development Plan of Jiangsu Province under Grant BE2017129.

ABSTRACT Active brake control systems are able to use more accurate control designs on the real-time knowledge of wheel slip such as tire braking forces and external momentums. A multi-objective Pareto type optimization approach is used to evaluate the inconsistent points of the optimization design namely those of minimizing the directional deviation while achieving maximum braking forces on wheels. Moreover, the optimal target slip values defined by the braking purposes like as shorter stopping distance and stability increment by keeping the vehicle in the straight line. This gets by the control of the longitudinal and lateral slip dynamics of each wheel concerning to the road conditions. A controller is optimally brought up by manipulating optimal control law with weights of two control inputs with mathematical and probabilistic characterization. The first-passage probability of critical response levels is used to directly control the vehicle directional stability. An impressive simulation technique based on Monte Carlo method named asymptotic sampling is applied to define the required first-passage probabilities and the Latin Hypercube sampling is used to design of experiments and to cover the design space. Afterwards, a Pareto-type optimization approach is applied to a trade-off between the inconsistent points of the optimization design. The simulation is conducted by the validated vehicle model and the results are indicated that the probability-based control design is represented as a preferable braking performance in comparison with the other systems for braking in sever conditions.

INDEX TERMS Brake by wire system, Latin hypercube sampling, Monte Carlo method, Pareto optimization, probability.

NOMENCLATURE

A_p	brake piston area
a_x	vehicle CG acceleration in the longitudinal direction
a_y	vehicle CG acceleration in the lateral direction
β_i	tire slip angle
β^*	generalized reliability index
$\beta^*_{w_u}$	corresponding reliability index
$\beta^*_{w_r}$	corresponding reliability index
C_{yi}	cornering stiffness of each tire
C_{xi}	longitudinal stiffness of each tire
D_F	failure region for the n-dimensional random variable space
δ_f	disturbance input
δ_i	front wheel steering angle
Δt	time intervals
e_i	tracking errors
f_0, f	initial factor
F_{xi}	longitudinal force
F_{yi}	lateral force
F_{yf}	mean values of front tire forces
F_{yr}	mean values of rear lateral tire forces
F_{zi}	normal load of tire
F_{zfl}	normal loads of left side for front wheels
F_{zrl}	normal loads of left side for rear wheels
F_{zfr}	normal loads of right side for front wheels
F_{zrr}	normal loads of right side for rear wheels
$F_z(t)$	vertical tire load
$F_{x(max)}$	force intensity
h	height of the sprung mass center of gravity
h_1	predictive period
h_2	predictive period
I_z	moment of inertia
$\dot{\lambda}_i$	longitudinal wheel slip lateral forces

The associate editor coordinating the review of this manuscript and approving it for publication was Hamid Mohammad-Sedighi.

m	vehicle mass
m_w	total mass of the tire and wheel
M_z	external yaw moment
μ_b	brake pad friction coefficient
μ	tire-road coefficient of friction direction
P_{bi}	braking actuator pressures
P_F	failure probability
r_d	desired value for the vehicle yaw rate
r_w	wheel radius on the pitch angle
s_i	tire longitudinal slip ratio
$\dot{\psi}$	yaw rate
$\ddot{\psi}$	angular acceleration
T_b	braking torque
T_w	track width
v_x	longitudinal velocity of the vehicle
v_y	lateral velocity of the vehicle
w_i	weighting ratio
w_r	weighting ratio related to the external yaw moment
w_u	weighting ratios related to the corrective
W_k	independent identically distributed (i.i.d.) random variables of the braking force
Ω	angular wheel velocity
X_i	random variables of braking forces
X_k	identically distributed Gaussian variables
χ	state vector
$\Phi^{-1}(\cdot)$	inverse standardized Gaussian distribution function

I. INTRODUCTION

Newly engineering science has benefited from probability knowledge with the safety approach. It has recognized and adopted concerning to accuracy and adaptability to be used in different subjects [1]–[5]. It has affected the process of developing technologies during the time periods of rapid developments [6]–[9]. On the other hand, the probability with safety approach incorporated with decision making are an intellectual method to analyze the engineering situations regarded as problems with uncertain input and output parameters and affects the outcomes while the action or process is not as anticipated [3], [10], [11]. Therefore, accountability of structural safety is necessary, and it can be provided by means of probability and decision making. The probability with safety approach is appropriate to use in new systems to make and preserve safety by moving toward a consistent point of possible ways [12], [13].

Although the braking system is designed for the safety of the vehicle, it can be possible to equip this system with protective designs to certify safety in braking situations entirely. Therefore, this aim may be achievable by conflicting between the optimal design objectives of an active braking system [14], [15]. Probabilistic base design and optimization can enable us to determine the probable optimal situations during the braking concerning to the random evolutionary operation of the braking [2], [16]–[19]. Solving this conflict can be possible by employing an accumulated weighting ratio to the particular objectives or a non-dominated resolution system which is-called Pareto set may be used [20]–[26]. The act of carefully pre-choosing of appropriate entrants is used to make a decision by the Pareto set [27]–[29]. Also, Pareto analysis tries to recognize and individuate the problems by utilizing the statistical methods and reach the optimum dealing with the difficult situation [30], [31]. Pareto analysis is an especial way of finding out the principal causes of difficult situations by using thought procedure simulation to indicate the schemes of repeated situations which stand in the way of making improvement of the situation [32], [33]. An efficient Monte Carlo based simulation [34]–[36]can be used to calculate the first passage probabilities [1], [17], [37]–[39]. Significant studies concerning the decision making and performing optimization process using random behaviour of actions have developed [1], [17], [21], [40], [41].

Recently, researchers in vehicle engineering are devised multicriteria Pareto optimization approaches for investigating the optimal decision tradeoffs [42]–[44]. The Pareto optimization framework considering discrepant driving schedules is used to evaluate the optimal fuel-cell durability in electric vehicles [42], [45]. The Pareto optimization of a five-degree of freedom vehicle vibration model is used to design an optimal vehicle vibration model [43], [46] and vehicle dynamics design [47].

Anti-lock braking system (ABS) is a famous active safety apparatus. It is so useful for severe braking situations. This system defines the minimum stopping distance by optimizing the value of the longitudinal wheel slip [48]. Also, the external yaw momentum is used to modify indirectly the vehicle directional stability [49], [50]. The conventional ABS just considered the longitudinal dynamics, in the way that the maximum force of braking is generated by the optimizing wheel slip in the longitudinal terms. So the conventional ABS is effective on the braking manoeuvre along a symmetric road. On the other hand, the braking manoeuvre on the asymmetric path like as a split-μ road creates an objectionable yaw moment on the vehicle because friction coefficient varies significantly on the right and left tires. The unexpected yaw moment causes the vehicle to deviate from the straight line and decrease the directional stability of the vehicle [51], [52]. Hence, preventing the vehicle deviation in braking manoeuvre and the minimum braking distance have the same important effect on the asymmetric road (split-μ) in hard braking which cannot be achieved entirely by the conventional ABS [53]. Therefore, braking on the split-μ road is considered in this paper to investigate and cover the most difficult braking situations.

It has shown that the control systems with wheel slip design are more proper to adjust the braking forces besides their adaptability to different vehicles, operating and road conditions [52], [54], [55]. Therefore, maximum braking force to achieve minimum stopping distance can be defined by keeping each wheel at a specified tire slip or optimally distribute on all wheels which is possible by using brake-by-wire

systems [56]–[58]. Referring to the brake-by-wire devices, they are categorized into two kinds: electro-hydraulic brake (EHB), and electro-mechanical brake (EMB) which employs the hydraulic and the electric power, respectively [59], [60]. Possibility of measuring the braking torque and braking pressure has used to define and calculate the tire braking force concerning the wheel dynamics.

On the other hand, the EHB brake by-wire systems are more comprehensive because of measuring the braking torque cannot be possible. As an alternative, measuring of the braking pressure concerning the brake disk-pad friction characteristics [61]–[63] have applied to the estimation of the braking force. In addition, brake pad wearing, brake ageing, heat, moisture and other probable process have a considerable effect on the friction characteristics [64]. So, in the EHB case, an adaptive control system is needed to adjust the wheel slip with respect to the control input which has formulated in terms of braking pressure, not braking torque and it is significantly affected by the road friction coefficient estimation and braking force which defined by a tire model with respect to the brake disk-pad friction variation.

The main objectives in previous studies are related to just minimizing the stopping distance, only keeping the directional stability of vehicle [65], [66]. Some researches include both goals by defining an extra wheel steering corrector for the braking system [67], [68]. Others have developed an integrated sliding base controller in order to reduce the undesired yaw moment [69] by controlling the longitudinal slip of each wheel separately on the split-μ road [70], [71] and different road surface conditions [72], [73]. This kind of controllers is worked through steer-by-wire, connected to conventional ABS. Furthermore, several studies are tried to use complementary condition of minimizing the lateral deviation in braking manoeuvre in the dynamics of system [74]. In another study, the H-infinity technique is used to design the steering controller compatible with the yaw moment generated through asymmetrically distribution of braking forces on a split-μ surface is proposed [75]. Some designs have developed the PID controller to apply the front wheel slip ratio for controlling the yawing motion during the braking on a split-μ road [76]. Also, some controllers are designed by concerning longitudinal and lateral dynamics and applying the extremum seeking algorithm to enhance the stability on hard braking condition [77].

In summary, research to design optimal and protective controllers has focused on investigating and conflicting between the braking parameters, which are creating the undesired moments to increase the stability and minimize the stopping distance. However, owing to the fact that integrated sliding base controllers optimize the braking operation and revenue, but itself is insufficient to accurately predict brake situations. Therefore a probabilistic base design and optimization method are used in this research to investigate and enhance the braking controller system through the Pareto approach and gain the optimum dealing at the severe braking situation which does not survey yet.

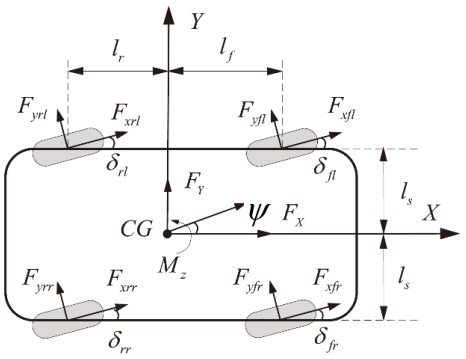

FIGURE 1. Vehicle model for four-wheel driving and steering [79].

The contribution of the research is to introduce and investigate a controller design by using the slip dynamics and Tire-road coefficient estimation and distribution of braking forces. Subsequently, a Pareto-type optimization approach on a probabilistic basis which is applied to the problem of optimizing the braking purposes like as shorter stopping distance and stability of the vehicle in the straight line during severe braking. The objective is formulated using an efficient computationally method conducted on probability-based design optimization of the active braking by wire system (especially EHB) on split-μ roads through developing Pareto based control system concerning enhancing the stopping distance and maneuverability of braking. Subsequently, an optimization procedure is applied with respect to the response surface approach and using an efficient Monte Carlo based simulation to calculate the first passage probabilities. Simulations are performed on the vehicle braking performance in different strategies which are without control, Stand-alone control, integrated control and probability control. Afterwards, the results of different strategies compared with the other control strategies to define the effeteness. Then a cost function based on Pareto analysis is constructed on the probability outcomes to put out a comprehensive compromise between conflicting optimization objectives in design.

This paper is organized as follows. Modelling of the vehicle and tire forces distributions and their dynamic systems are presented in section II. A nonlinear controller is designed for controlling the sliding modes by presenting the slip dynamics in section III. Tire-road coefficient estimation is conducted in section IV. A nonlinear controller for evaluating the external yaw moment is designed in section V concerning to determine a target for external yaw moment by designing an optimal algorithm for distribution of braking forces. In section VI, the reliability model is designed and conducted to the braking system problem. The results of simulations are presented in section VII and are enhanced by using real-time tire-road friction conditions. The results are presented and evaluated for braking control design and reliability control design and followed by the Pareto optimization. In section VIII, the conclusive remarks are presented.

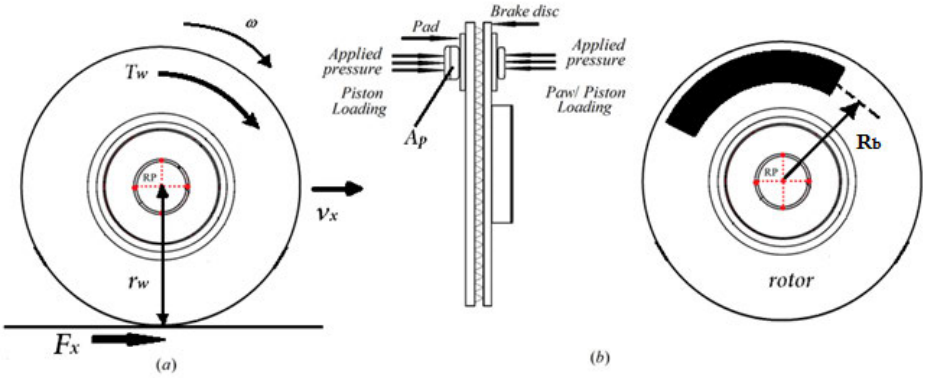

FIGURE 2. (a) Force diagram of a wheel, (b) hydraulic disc brake diagram [80], [81].

II. VEHICLE AND TIRE BRAKING FORCE MODELLING

A vehicle dynamic model with five degrees of freedom, including lateral, longitudinal, and yawing movements, which has been experimentally validated [78], is employed. Since the focus of this research is on braking control for stopping distance and lateral stability, pitch, roll, and vertical motions are ignored. The vehicle dynamic equations of motion are given as follows. The force diagram of the vehicle model is illustrated in Figure 1.

$$\begin{aligned} m\left(\dot{v}_x - \dot{\psi} v_y\right) &= \sum_{i=1}^{4}\left(F_{xi}cos\delta_i\right) + \sum_{i=1}^{4}\left(F_{xi} - F_{yi}sin\delta_i\right) \\ m\left(\dot{v}_y + \dot{\psi} v_x\right) &= \sum_{i=1}^{4}\left(F_{xi}sin\delta_i\right) + \sum_{i=1}^{4}\left(F_{yi}cos\delta_i + \left(F_{xi}\right)\right) \\ I_z\ddot{\psi} &= \sum_{i=1}^{4}(-1)^i l_s\left(F_{xi}cos\delta_i - F_{yi}sin\delta_i\right) \\ &\quad + \sum_{i=1}^{2} l_f\left(F_{xi}cos\delta_i + F_{yi}sin\delta_i\right) \\ &\quad - \sum_{i=1}^{4} l_y\left(F_{xi}cos\delta_i + F_{yi}sin\delta_i\right) + M_z \end{aligned} \quad (1)$$

where I_z and m are the mass moment of inertia and mass of the vehicle, respectively. v_x, v_y represent the longitudinal and lateral velocities of the vehicle, and F_{xi}, F_{yi} indicate the forces in longitudinal and lateral directions for the i th tire, respectively, with the specification for each wheel as $i = 1 = fl, i = 2 = fr, i = 3 = rl, i = 4 = rr$. The yaw rate is shown by $\dot{\psi}$, the angular acceleration is $\ddot{\psi}$ and δ_i expresses the angle of steering for the ith wheel. Concerning F_{yl} and F_{yr} are the mean values of front and rear lateral tire forces with equations:

$$\begin{cases} F_{yf} = \dfrac{\left(F_{yfl} + F_{yfr}\right)}{2} \\ F_{yr} = \dfrac{\left(F_{yrl} + F_{yrr}\right)}{2} \end{cases} \quad (2)$$

The tire force in the longitudinal direction is generated by employing braking in the wheel and the friction generated between the surface of the road and a tire, as shown in Figure 2(a). Concerning the hydraulic braking system, it is possible to define the wheel torque through the parameters and the pressure of brake, see Figure 2(b).

$$T_{wi} = -2P_{bi}A_{pi}R_{bi}\mu_b \quad (i = 1\ to\ 4) \quad (3)$$

The average value of the brake pad friction coefficient of all disk brakes represented by μ_b and A_p is the area of brake piston. Concerning Eq. (3) the dynamics equations of the wheel can be rewritten as follows:

$$J_{wi}\dot{\omega}_i = T_{wi} - r_w F_{xi} = -2P_{bi}A_{pi}R_{bi}\mu_b - r_w F_{xi} \quad (4)$$

III. SLIP DYNAMICS AND DESIGN OF NONLINEARSLIDING MODE CONTROLLER

The longitudinal wheel slip controller has designed concerning a nonlinear model for four wheels of the vehicle with 5-DOF constitute of vehicle velocity in the longitudinal direction and all four wheels rotational speed. Estimation of friction between the disk and pad and force of tires is done by the monitoring model concerning the friction variation between the brake disk and pad. The unknown variables in the nonlinear vehicle model as represented in Eqs. (1) and (4) are the longitudinal tire forces F_{xi}, lateral tire forces F_{yf}, F_{yr} and brake disk-pad friction coefficient μ_b which it is hard to measure by physical sensors. Estimation of these unknown variables is possible by augmenting them as state variables in the state equation. The derivatives in terms of time for the augmented variables are supposed to be zero. Therefore, observing model is defined concerning the nonlinear state Eqs. (1) and (4):

$$\dot{\omega}_i = \frac{-2P_{bi}A_{pi}R_{bi}\mu_b - r_w F_{xi}}{J_{wi}} \quad (i = 1\ to\ 4) \quad (5)$$

$$\begin{cases} \dot{\mu}_b = 0 \\ \dot{F}_{xi} = 0 \quad (i = 1\ to\ 4) \\ \dot{F}_{yf} = 0 \\ \dot{F}_{yr} = 0 \end{cases} \quad (6)$$

The output variables of the observing model are represented in the output Eq. (7) which are the accelerations in longitudinal and lateral directions, yaw rate, and velocities of

four wheels.

$$\mathbf{u}=\begin{bmatrix}\mathbf{a_x}\\ \mathbf{a_y}\\ \dot{\psi}\\ \boldsymbol{\omega_1}\\ \boldsymbol{\omega_2}\\ \boldsymbol{\omega_3}\\ \boldsymbol{\omega_4}\end{bmatrix}=\begin{bmatrix}\frac{1}{m}\left(\sum_{i=1}^{4}(F_{xi}cos\delta_i)\right.\\ \left.+\sum_{i=1}^{4}(F_{xi}-F_{yi}sin\delta_i)\right)\\ \frac{1}{m}\left(\sum_{i=1}^{4}(F_{xi}sin\delta_i)\right.\\ \left.+\sum_{i=1}^{4}(F_{yi}cos\delta_i+(F_{xi})\right)\\ \dot{\psi}\\ \omega_1\\ \omega_2\\ \omega_3\\ \omega_4\end{bmatrix} \tag{7}$$

The tire forces is considered to define by the tire brush model [73] with the assumption of small longitudinal slip. The tire forces are defined by assuming there is no coupling relationship between the tire forces in the longitudinal and lateral directions as follows:

$$\begin{cases}F_{xi}=C_{xi}s_i-\frac{1}{3}\frac{(C_{xi}s_i)^2}{\mu F_{zi}}+\frac{1}{27}\frac{(C_{xi}s_i)^3}{(\mu F_{zi})^2}\\ F_{yi}=2\mu F_{zi}\left\{\begin{array}{l}\left|\frac{C_{yi}}{tan}\beta_i\mu F_{zi}\right|-\\ \frac{1}{3}\left|\frac{C_{yi}tan\beta_i}{\mu F_{zi}}\right|^2+\\ \frac{1}{27}\left|\frac{C_{yi}tan\beta_i}{\mu F_{zi}}\right|^3\end{array}\right\}\mathrm{sgn}\,(\beta_i)\,,\\ \qquad\left|\frac{C_{yi}}{tan}\beta_i\mu F_{zi}\right|\le 3\end{cases} \tag{8}$$

where, C_{yi} and C_{xi} are represented the cornering stiffness and the longitudinal stiffness for tires, respectively. The tire longitudinal slip ratio is represented by s_i and β_i indicates the slip angle of the tire. The coefficient of friction between tire and road and the normal load of tire are represented as μ and F_{zi} respectively. Since the parameters of vehicle are identified, the normal tire loads can be defined as:

$$\begin{cases}F_{zfl}=m_wg+\dfrac{Mgl_r-Mha_x-Mha_yl_r}{2(l_r+l_f)}\\ F_{zrl}=m_wg+\dfrac{Mgl_r+Mha_x-Mha_yl_r}{2(l_r+l_f)}\\ F_{zfr}=m_wg+\dfrac{Mgl_r-Mha_x+Mha_yl_r}{2(l_r+l_f)}\\ F_{zrr}=m_wg+\dfrac{Mgl_r+Mha_x+Mha_yl_r}{2(l_r+l_f)}\end{cases} \tag{9}$$

where, $F_{zfl}, F_{zrl}, F_{zfr}, F_{zrr}$ are the normal loads of left and right side for front and rear wheels respectively. The total mass of the wheel and the height of the sprung mass centre of gravity are represented by m_w and h, respectively. The vehicle CG acceleration in the longitudinal and lateral directions are represented by a_x, a_y. The relative difference between the longitudinal vehicle velocity and the wheel velocity is used to define the wheel slip. It generated between a tire and road surface during braking and is defined as:

$$\lambda=\frac{v_x-r_w\omega}{v_x} \tag{10}$$

The slip dynamics equation is defined by differentiating Eq. (10) and substituting Eq. (4) as follows:

$$\dot{\lambda}=-\frac{\dot{v_x}}{v_x}(\lambda-1)-\frac{r_w}{J_wv_x}(r_wF_b-2P_bA_pR_b\mu_b) \tag{11}$$

The EHB actuator pressure of each tire is used to design the control system as the control input to drive the wheel slip and the target point. Therefore, to get this purpose, a predictive method will be used to design an optimal nonlinear control law.

The nonlinear vehicle model with 5-DOF defined by Eqs. (1) and (11) can be expressed in the state space form. Using Eq. (1) the longitudinal motion can be written as $m\dot{u}=\sum F_{xi}$, where u is the longitudinal velocity, F_{xi} is the longitudinal tire force and m is the total mass of the vehicle. Considering the longitudinal slip of each tire as the outputs of the system, it can be written:

$$\begin{cases}\dot{\chi}_1=f_1(\chi)\\ \dot{\chi}_i=f_i(\chi)+\dfrac{r_w}{J_w\chi_1}T_{bi}\quad(i=2\ to\ 5)\end{cases} \tag{12}$$

using Eq. (4) gives:

$$\dot{\chi}_i=f_i(\chi)+\frac{r_w}{J_w\chi_1}T_{bi}\quad(i=2\ to\ 5) \tag{13}$$

where the nonlinear tire brush model has been incorporated in f_1 and f_i. It should be mentioned that the system outputs are considered as the tires longitudinal slip. Concerning equation $T_b=2P_bA_pR_b\mu_b$ we can write:

$$\dot{\chi}_i=f_i(\chi)+\frac{2A_{pi}R_{bi}\mu_{bi}r_w}{J_w\chi_1}P_{bi}\quad(i=2\ to\ 5) \tag{14}$$

$$\dot{\chi}_i=f_i(\chi)+\frac{r_w}{J_w\chi_1}\left(r_wF_b+\frac{J_w\dot{v}_x}{r_w}(\lambda-1)\right)\quad(i=2\ to\ 5) \tag{15}$$

$$\mathbf{u}=[\chi_2\quad\chi_3\quad\chi_4\quad\chi_5] \tag{16}$$

where the state vector represents by $\chi=[v\lambda_{2(fL)}\ v\lambda_{3(rL)}\ v\lambda_{4(fR)}\ v\lambda_{5(rR)}]$ and the outputs vector is $\mathbf{u}$. The braking actuator pressures are expressed by P_{bi} as the control inputs. Concerning Eq. (8), the nonlinear brush tire model has been used to define F_{xi} and F_{yi}. The Taylor series expansion is used to anticipate the next time interval of nonlinear responses of vehicle, $\chi_i(t+h_1)$. Subsequently, a minimization method is applied continuously to estimate tracking errors and finally defining the current control $P_{bi}(t)$. On the other hand, h_1 is the predictive period and a real positive number. Hence, to assess the next instant tracking errors, a performance index with respect to the point-wise minimization process is needed which is written as:

$$J_1\left[P_{bi}(t)\right]=\frac{1}{2}\sum_{i=2}^{5}w_ie_i^2(t+h_1)\quad(i=2\ to\ 5) \tag{17}$$

where, weighting ratios and tracking errors are denoted by w_i and e_i, respectively. e_i can be determined as follows:

$$e_i(t+h_1) = \chi_i(t+h_1) - \chi_{id}(t+h_1) \tag{18}$$

It can be seen that the performance index does not have the control inputs weighting condition in case of complete tracking because the control inputs P_{bi} have no limitation, and this case remarked as the cheap control [82], [83]. In this situation regarding nonlinear brush tire model and its force capability, the brake pressure can be assigned to reach the maximum achievable braking force and its amount will be in an acceptable range to be employed. The performance index Eq. (17) can be expanded as a function of the control input. Therefore for each tire, the longitudinal slip response should be defined in the next time interval. Hence, a Taylor series of qth-order at t term is used to approximate of each $\chi_i(t+h_1)$ as follows:

$$\chi_i(t+h_1) = \chi_i(t) + h_1\dot{\chi}_i(t) + \frac{h_1^2}{2!}\ddot{\chi}_i(t) + \cdots + \frac{h_1^q}{q!}\chi_i^{(q)}(t) \tag{19}$$

The expansion order q determines the highest order derivative for each output in estimation and is applied to attain the minimum control effort concerning to the nonlinear system relative degree [84]. It can be seen that the well-defined relative degree of the system has a value of $\rho = 1$ for all the outputs. Concerning the inputs first appear explicitly, the outputs are determined by the derivatives at the lowest order. Therefore, the first-order Taylor series is useful and adequate to expand the outputs.

$$\chi_i(t+h_1) = \chi_i(t) + h_1\dot{\chi}_i(t) \tag{20}$$

Eq. (9) can be rewritten concerning to Eq. (4) as:

$$\chi_i(t+h_1) = \chi_i(t) + h_1\left(f_i + \frac{2A_{pi}R_{bi}\mu_{bi}r_w}{J_w\chi_1}P_{bi}\right) \tag{21}$$

In the same way, the desired longitudinal wheel slips are expanded as:

$$\chi_{id}(t+h_1) = \chi_{id}(t) + h_1\dot{\chi}_{id}(t) \tag{22}$$

Substituting the Eqs. (14) and (22) into Eq. (17) gives the function of control input which results from the expansion of performance index. Using the optimal condition:

$$\frac{\partial J_1}{\partial P_{bi}} = 0 \tag{23}$$

gives the braking pressure control laws for four wheels:

$$P_{bi} = -\frac{J_w\chi_1}{2A_{pi}R_{bi}\mu_{bi}r_w}\left[e_i + h\left(f_i - \dot{\lambda}_i\right)\right] \quad (i = 2\ to\ 5) \tag{24}$$

The conventional ABS controller try to define the longitudinal wheel slip ($\dot{\lambda}_i$) at the proper value for each tire, then using the braking forces at the maximum level can be possible during the braking. Therefore, it can be seen that particular longitudinal slip values lead to the tire force at the maximum level, which can be called the optimum wheel slip. Easily differentiation of the longitudinal force in terms of the wheel slip ratio leads to the optimum value for each tire as follows [84]:

$$\left.\frac{\partial F_{xi}}{\partial \lambda_i}\right|_{\lambda_i} = 0 \tag{25}$$

where, F_{xi} is the tire force in a longitudinal direction and has been defined by the brush tire model Eq.(10). Dependence of the optimum wheel slip on the tire model precision can be lead to inexact determination in practice which is affected by uncertainties in its parameters or discrepancies of tire model. As regards, updating the reference wheel slip in this way is more effective in comparison with considering all conditions with a constant reference wheel slip. Therefore, enhanced performance can be achieved by the accurate recognition of tire model parameters. On the other hand, on a split-μ road and severe braking situation, the optimum distribution of tire forces should be used to define the desired longitudinal slip value for tires separately. Thus, external yaw moment will be turned out due to decrease in amount of maximum braking force of tires individually, and it tries to keep the vehicle on the straight line whenever reaching to shorter stopping distance.

IV. TIRE –ROAD FRICTION COEFFICIENT ESTIMATION

The active vehicle control system can be enhanced by the valuable source of information which provided by the capability in predicting the friction coefficient in real-time conditions to increase the proficiency of systems using wheel slip control [55], [77]. Estimation of the wheel slip value can be dealing with the ability to recognize the peak of the tire-road friction curve combined with the capability of identifying. The full parameterization of the tire-road friction curve itself is needed. Particularly, a properly parameterized friction model can be applied to formulate of the curve fitting solution in the identification approach—the curve fitting estimation use to define the slip value compatible with the curve peak. The Burckhardt friction model [85] is applied to achieve this goal.

The identification problem can be established by the available variables ω, v_x, λ and T_b. The longitudinal tire-road force is obtained by the assumption of the proportional relationship between the normal force and longitudinal force [85]:

$$F_x = F_z\mu(\lambda) \tag{26}$$

Considering different road conditions can be varied the $\mu(\lambda)$, Eq. (11) can be written as:

$$\dot{\lambda} = -\frac{1}{v_x}\left(\frac{(1-\lambda}{m} + \frac{r_w^2}{J_w}\right)F_z\mu(\lambda) - \frac{2r_w}{v_xJ_w}P_bA_pR_b\mu_b \tag{27}$$

Suitable data collection for the tire-road friction curve $\mu(\lambda)$ estimation can be found by inverting Eq. (27) to achieve data points of type $\mu(\omega, v_x, T_b, \lambda)$. It should be noted that the braking torque T_b can be defined concerning to proportionality to the pressure in the hydraulic braking circuit

(if v_x cannot be defined directly and needs to be estimated). Angular wheel velocity ω can be assumed to be able to be measured. Then, λ can be defined concerning the ω and v_x. Substituting $\omega r/(1-\lambda)$ as v_x with respect to Eq. (27) gives $\mu(\lambda)$ as:

$$\mu(\lambda;t) = \frac{\frac{-2(1-\lambda(t))P_b(t)A_pR_b\mu_b}{J_w\omega(t)} - \dot{\lambda}(t)}{\frac{1-\lambda(t)}{r_w\omega(t)}F_z(t)\left(\frac{1-\lambda(t)}{m} + \frac{r_w^2}{J_w}\right)} \tag{28}$$

where the dependence on time is made explicit in order to point out that Eq. (28) holds at each time instant. Concerning the dependence on $\omega(t)$, $\lambda(t)$, $\dot{\lambda}(t)$, r_w and $P_b(t)$, the noise-free measurements of such variables can be lead to exact estimation of $\mu(\lambda;t)$. It should be noted that Eq. (28) is affected by the error estimation which comes from noisy sensors using to measure $\omega(t)$ and $P_b(t)$, speed estimation using to define $\lambda(t)$, the dependence of the vertical load $F_z(t)$ and the wheel radius r_w on the pitch angle and tire characteristics (which vary from the static value). Also, it can be seen from the Eq. (8) (the longitudinal tire force model), the vertical load $F_z(t)$ can be considered as a measuring factor on the curve of friction and subsequently do not affect the maximum point. Consequently, it has been found that Eq. (28) is a nonlinear function that depended on data and noise and noisy estimation of $\mu(\lambda;t)$ can be determined. Therefore, Burckhardt model used to prepare appropriate parameterizations which can be applied to formulate the tire-road friction relation and found the curve-fitting problem. The Maximum Likelihood Approach (ML approach) is used to fit the tire-road friction curve in identification strategy. The method applied the fitting error criterion with an iterative minimization by means of a quasi-Newton method which is explained in appendix.

V. EXTERNAL YAW MOMENT-NONLINEAR CONTROLLER DESIGN

The lateral vehicle dynamics can be defined by the nonlinear 5-DOF four-wheel model and has applied to stabilize the vehicle-handling dynamics and set up the external yaw moment controller. The degrees of freedom considered as the lateral velocity and yaw rate, recalling from Eq. (1) the equations of motion governed as:

$$\begin{aligned}
\dot{v}_y &= -\dot{\psi}v_x + \frac{1}{m}\left(\begin{array}{l}\sum_{i=1}^{4}(F_{xi}sin\delta_i) \\ +\sum_{i=1}^{4}(F_{yi}cos\delta_i + (F_{xi})\end{array}\right) \\
\ddot{\psi} &= \frac{1}{I_z}\left[\begin{array}{l}\sum_{i=1}^{4}(-1)^i l_s\left(F_{xi}cos\delta_i - F_{yi}sin\delta_i\right) \\ +\sum_{i=1}^{2}(l_f F_{xi}cos\delta_i + F_{yi}sin\delta_i) \\ -\sum_{i=1}^{4}(l_y F_{xi}cos\delta_i + F_{yi}sin\delta_i) + M_z\end{array}\right]
\end{aligned} \tag{29}$$

where $\dot{\psi}$ and δ_i are represented for the yaw rate and the steering angle of front wheels. v_x is the lateral velocity and F_{xi} and F_{yi} is the longitudinal and lateral tire forces respectively (have been described by the brush tire model Eq.(8)). The differential longitudinal forces produce the required external yaw moment, represented by M_z and it should be defined by the control law. The lateral velocity in Eq. (29) can be written in the normal case to consist of the vehicle side-slip angle ($\beta = v_y/v$). Subsequently, outputs of the system can be considered as the tires longitudinal slip respectively and it is thus possible to write the equations in the state space form. Denote $\chi = [u\lambda_1\ \lambda_2\ \lambda_3\ \lambda_4]$ as the state vector, where u is the forward velocity and λ_i are longitudinal wheel slips, it can be defined:

$$\dot{\chi}_1 = \kappa_1(\chi, \delta_f) \tag{30}$$

$$\dot{\chi}_1 = \kappa_2(\chi, \delta_f) + \frac{M_z}{I_z} \tag{31}$$

$$\mathbf{u} = [\chi_1\ \chi_2\ \chi_3\ \chi_4] \tag{32}$$

where $\boldsymbol{u}$ is the system output vector. M_z is the external yaw moment control input and δ_f is the disturbance input. κ_1 and κ_2 are denoted the nonlinear brush tire model. Using the same procedure as has been used for the ABS slip controller design by the prediction method, leads to define external yaw moment by a nonlinear control law in optimal condition. Therefore M_z is the control input and considered as weighting ratio. It is incorporated in the index of performance in contrast with the ABS slip controller design. In this case, the maximum braking forces should not be decreased inordinately, and the lowest value of external yaw moment needed to be considered. On this point of view, this case is supposed to be as expensive control. The yaw rate seeking inaccuracy at the next instance and the control consequence are assessed by the pointwise minimization performance index as follows:

$$J_2[M_z(t)] = \frac{1}{2}w_r\left[\dot{\psi}(t+h_2) - \dot{\psi}_d(t+h_2)\right] + \frac{1}{2}w_u\left[M_z^2(t)\right] \tag{33}$$

where weighting ratios are presented by w_r and w_u and related to the external yaw moment and the corrective lateral forces of the wheels. They use to define the relative error and the required force in minimizing the performance index. Predictive period is h_2 and $\dot{\psi}_d$ is the proper yaw rate value for the vehicle. In the manoeuvring in the straight line, $\dot{\psi}_d$ is equal to zero. Applying a similar way like as the ABS design, Taylor series is used to define the responses of the system and subsequently, the control input M_z is employed to define the performance index Eq. (33). Hence, the optimal condition is applied:

$$\frac{\partial J_2}{\partial M_z} = 0 \tag{34}$$

and resulted to:

$$M_z(t) = -\frac{I_z}{h_2(1+\gamma I_z^2 h_2^{-2})}\left[e_{\dot{\psi}} + h_2(\kappa_2 - \ddot{\psi}_d)\right] \tag{35}$$

where the tracking error of the current yaw rate represented by $e_{\dot{\psi}}$ and can be demonstrated as:

$$e_r(t) = \dot{\psi}(t) - \dot{\psi}_d(t) \tag{36}$$

also, γ is the weighting ratio and considered as:

$$\gamma = \frac{w_u}{w_r} \geq 0 \tag{37}$$

It can be seen that the external yaw moment can be adjusted concerning the weighting ratio value. The limit situations are indicated that the external yaw moment is zero ($M_z(t) = 0$) when $\gamma = \infty$, and mutually considering $\gamma = 0$, there is no decrease in the value of control input and the tracking can be achieved in a perfect way. These cases are considered as expensive and cheap controls, respectively. Thus, the tracking accuracy can be made a deal with the control energy concerning the adjustable parameter γ in the control law.

A. DETERMINATION OF EXTERNAL YAW MOMENT TARGET

It has been shown that the weighting ratio γ affects the control inputs and uncertainties of modelling. The effects of these parameters can be defined concerning to effects on the control performance. Therefore, the nominal based control law Eq. (35), is applied to the actual model Eq. (30) as follows:

$$\ddot{\psi} = \kappa_2 - \frac{1}{h_2(1+\gamma I_z^2 h_2^{-2})}\left[e_{\dot{\psi}} + h_2(\hat{\kappa}_2 - \ddot{\psi}_d)\right] \tag{38}$$

It should be noted that the symbol "^" is used to indicate the nominal model. The yaw rate tracking error dynamics can be defined by using a manipulated way in writing the derived Eq. (38) as:

$$\left(\dot{e}_{\dot{\psi}} + \frac{1}{h_2(1+\gamma I_z^2 h_2^{-2})}\right) e_{\dot{\psi}} = (\kappa_2 - \hat{\kappa}_2) + \left(1 - \frac{1}{(1+\gamma I_z^2 h_2^{-2})}\right)(\hat{\kappa}_2 - \dot{\psi}_d) \tag{39}$$

Mentioning that errors of estimation, unmodeled dynamics and changes in the parameters of vehicle dynamics can deviate $\hat{\kappa}_2$ from the nominal model. On the other hand, $\hat{\kappa}_2$ has a proportional relation to the internal yaw moment, which is resulted of tire lateral force. Concerning the saturation of tire force, it can be realized that function $\hat{\kappa}_2$ is bounded and the constants $S_1 > 0$ and $S_2 > 0$ can be considered as $|\kappa_2 - \hat{\kappa}_2| \leq S_1$ and $|\hat{\kappa}_2 - \ddot{\psi}_d| \leq S_2$. Rewriting Eq. (39) using the bounds to the error dynamics leads to:

$$\left(\dot{e}_{\dot{\psi}} + \frac{1}{h_2(1+\gamma I_z^2 h_2^{-2})}\right) e_{\dot{\psi}} \leq S_1 + \left(1 - \frac{1}{(1+\gamma I_z^2 h_2^{-2})}\right) S_2 \tag{40}$$

Applying zero initial condition to the first-order differential equation gives the tracking error limits as:

$$-e_m \leq e_{\dot{\psi}} \leq e_m \quad forall\ t \geq 0 \tag{41}$$

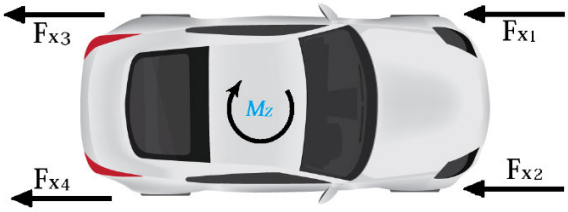

FIGURE 3. Distribution of braking forces on the vehicle sides.

where

$$e_m = \left(1 + \gamma I_z^2 h_2^{-2}\right) F h_2 + (\gamma I_z^2 h_2^{-2}) h_2 S_2 \tag{42}$$

Afterwards, it is possible to define the tracking error limits with the weighting ratio γ terms:

$$e_m = S_1 h_2 + \frac{\gamma}{h_2} I_z^2 (F + S_2) \tag{43}$$

Eq. (43) shows that the control input reduces by the tracking error where the uncertainties of the modeling function S_1 and the weighting ratio γ generate the tracking error. Especially if there is no decrease in control input and indeterminacy of the modelling, it can be possible to define the yaw rate tracking error by:

$$\dot{e}_{\dot{\psi}} + \frac{1}{h_2} e_{\dot{\psi}} = 0 \tag{44}$$

Considering Eq. (44), a particular linearized case of input/output has defined which indicate that yaw rate perfect tracking is retained for all t, because the initial yaw rate tracking error has zero value. Therefore, all $h_2 \geq 0$ provided the linear and exponentially stable system.

B. AN ALGORITHM FOR DISTRIBUTION OF BRAKING FORCES

In the present research, the split-μ road is considered because the road may be perceived as hazardous when the vehicle accelerating, cruising or braking hardly. Therefore an algorithm is propounded to indicate the distribution of braking forces properly on the split-μ road condition. The maximum braking forces $F_{xi(max)}$ $(i = 1, 2, 3, 4)$ and the stabilizing yaw moment M_z are the inputs of the algorithm which defined by the conventional ABS relations and the control law Eq. (35), respectfully. The outputs can be determined concerning getting the minimum stopping distance and minimum deviation in braking manoeuvring. The braking forces of wheels $F_{xi(max)}$ $(i = 1, 2, 3, 4)$ are distributed (Figure 3) and are defined in the optimal condition and gives the outputs. Therefore, at the situation, there is no reduction in the braking forces and they are at maximum amounts, the differential longitudinal forces try to provide the $M_{z(max)}$ as follows:

$$M_{z(max)} = \left[\begin{matrix}\left(F_{x2(max)} + F_{x4(max)}\right) - \\ \left(F_{x1(max)} + F_{x3(max)}\right)\end{matrix}\right] \frac{T_w}{2} \tag{45}$$

The track width is shown by T_w and according to the load transferring in the longitudinal and lateral directions in

manoeuvres, the tires have different maximum forces. Subsequently, a comparative scale concerning the external yaw moment $M_{z(max)}$ with the required yaw moment M_z (defined by control law Eq. (35)) can be applied which three cases can be predicted:

Case I($M_{z(max)} = M_z$): is the ideal situation and the maximum braking forces are not decreased to provide the necessary stabilizing yaw moment, it means $F_{xi} = F_{xi(max)}$ $(i = 1, 2, 3, 4)$.

Case II($M_{z(max)} < M_z$): the necessary yaw moment is provided by decreasing the one side forces. Thus, the forces of F_{x2} and F_{x4} should be preserved at their maximum values $F_{xi} = F_{xi(max)}$ $(i = 2, 4)$ and on the other hand F_{x1} and F_{x3}, are decreased to remunerate the necessary yaw moment. The relation between the forces to define the reduced forces is as follows:

$$M_{z(max)} = \left[\left(F_{x2(max)} + F_{x4(max)}\right) - \left(F_{x1} + F_{x3}\right)\right] \frac{T_w}{2} \tag{46}$$

M_z computed by using the control law. At first step Eq. (46) can be computed for the forces F_{xi} $(i = 1, 3)$. Since the load transfer is conducted from the rear axle to the front, F_{x3} is chosen to decrease and F_{x1} is put at the maximum value $F_{x1} = F_{x1(max)}$. For more decrement, it can be possible by setting F_{x3} to zero and define the F_{x1} by the Eq. (48). On the other hand, setting the zero value for F_{x1} and F_{x3} and the maximum value for F_{x2} and F_{x4}, leads to the maximum yaw moment.

Case III($M_{z(max)} > M_z$): in this case, the position of the braking forces on the wheels will be shifted on the other side and other processes are the same.

It should be noted that concerning to vehicle model (Fig. 1), the force distribution can be shown as $F_{x1} = F_{xfl}, F_{x2} = F_{xfr}$, $F_{x3} = F_{xrl}, F_{41} = F_{xrr}$.

VI. RELIABILITY MODEL

Higher accuracy and robustness in the braking distribution algorithm can be achieved by performing a compromised optimization procedure on the inputs and outputs of algorithm which inputs are braking forces at maximum values, the stabilizing yaw moment (M_z) and the outputs are the stopping distance and the directional stability. The braking forces are modelled as non-stationary random variables. Hence, the braking distribution algorithm design can be possible using a proper dynamic response characterization by the probabilistic process, such as the first-passage critical response probability. In this scenario, to achieve minimum braking distance meanwhile adjusting and regulating the yaw rate at zero value and confining the angle of side-slip, the steering and braking controls should be allied to decrease the contribution of the external yaw moment.

In general, random variables $x_1, \cdots, x_n$ with an n-dimensional space have the failure probability of P_F as [86]:

$$P_F = \int_{D_F} f_{x_1,\cdots,x_n}(x_1, \cdots, x_n) dx_1 \cdots dx_n \tag{47}$$

where $f_{x_1,\cdots,x_n}(x_1, \cdots, x_n)\, dx_1 \cdots dx_n$ denotes the joint probability function of the random variables $x_1, \cdots, x_n$. The failure region for the n-dimensional random variable space is represented by D_F and is called the failure domain. According to the first-passage probability principle, the first response value which occurs largely than an assigned threshold n is considered as failure. Therefore, the generalized reliability index β^* is introduced as:

$$\beta^* = \Phi^{-1}(1 - P_F) \tag{48}$$

where $\Phi^{-1}(\cdot)$ denotes the inverse of the standardized Gaussian distribution function. The random variables X_i (braking distance) are considered to be Gaussian. They are distributed with zero mean and standard deviation σ and are independent.

Assuming a limit state function $g(X)$ possibly highly nonlinear and the failure can be indicated by $g < 0$. Consider the standard deviation of the identically distributed Gaussian variables X_k; $k = 1, 2 \ldots, n$ as σ. A suitable sampling technique can be tried to define the functional dependency between the generalized safety index β^* and the standard deviation σ. In order to get this aim, some limited cases of analytical considerations can be used.

The assessment of first-passage probabilities in random braking can be possible by applying frequently applied approach based on the first-order reliability method [2], [38]. This approach can be further elevated by the importance of sampling [87], [88]. Concerning the first-order reliability method (FORM) [89]–[91], the linearized limit state function [22] with respect to the most probable failure point is used to define the probability of failure. The failure condition in the standard Gaussian spaces $g(u^*) \leq 0$, where the u^* is represented the most probable failure point and has the minimum deviation β^* with respect to the source of origination. Consider braking issue; it is possible to call this as the braking design point in the first-passage problem [75], [87], [92]–[94]. As regards in order to conduct the problem, the optimization procedure should be applied to define u^* and β^*. It should be noted that the optimization procedure may converge so slowly or the global minimum point does not converge with respect to the considered algorithms [95]–[99] which can be tested for the present application. In this case, to demonstrate the braking forces with adequate accuracy, an enormous number of random variables are needed. Even though the successful convergence can be achieved, but the computational process is considerable. Estimation of one gradient needs nonlinear dynamic analyses with employing a large number of resolution. Concerning the computation process particularly for gradient estimation indicate that applying FORM to define the safety indices concerning the space design of the variables M_z thoroughly and γ seems to be not conceivable.

Thus, an asymptotic sampling method [1] based on the Monte-Carlo approach [100] is used to rapidly determine the first passage reliability safety indices. This method considered in n-dimensional identically distributed Gaussian space, it depends on the asymptotic behaviour of the failure

probability concerning σ as the variables standard deviation. Subsequently, zero failure probability is achieved [101]. The dimensional independence of this method has a significant advantage. The accuracy can be controlled with respect to the specific limit state surface geometry $g(u) = 0$, the samples quantity and the failure probability. It can be seen that, using an extrapolation method, can be utilized the asymptotic behaviour of the safety index β^* in asymptotic sampling concept. Here, dependency of β^* and the random variables standard deviation σ can be indicated functionally as:

$$\beta^* = A.f + \frac{B}{f}; \quad f = \frac{1}{\sigma} \tag{49}$$

It can be seen that when $f \to 0$, the necessary asymptotically linear behaviour can be satisfied by concerning that $\sigma \to 0$. The regression analysis with commonly least-squares fitting is used to define the coefficients A and B based on Monte Carlo estimations of β^* for different values as support points. We can modify the fitting procedure with respect to the scaled safety index by Eq. (49) as:

$$\frac{\beta^*}{f} = A + \frac{B}{f^2} \tag{50}$$

Rewriting Eq. (49) allows the regression analysis to present identical weights for all support points (Figure 5). The principal steps of the asymptotic sampling method is shown as a flow chart in Figure 5. Paying attention to the algorithm at first an initial factor f_0 is selected and because of the absence of any previous information, the helpful set is to consider $f_0 = 1$. The other important measurable factor is N_0 which represents the quantity of failure domain samples, because safety index $\beta^*(f)$ accuracy is affected by the number of samples. Normally in primary steps, the real samples number N_F will be so small in the failure domain. Therefore, in this situation, the factor f start to be reduced ($f = 0.9$ or less factors) until acceptable large N_F can be reached by repeating the simulation procedure. Also, simulations and decreasing way of f is followed until adequate number k concerning pairs f and β^* can be achieved. In this research, $N_0 = 10$ and $k = 5$ have been chosen. After the determination of the parameters, applying a regression on the data pairs gives the function relation $\beta^*(f)$. Extrapolating $\beta^*(f)$ to $f = 1$ results to the safety index as shown in Figure 4. More information on different applications and the accuracy of the method has been discussed in [1], [21], [99].

On the other hand, concerning applying this method in braking scenario and braking simulations, the continuous time for braking periods should be discretized. This can be defined by representing the braking force by a sequence of independent identically distributed (IID.) random variables W_k. It is supposed that the random variables have a constant amount with respect to Δt time intervals. The variables W_k have zero mean and a variance $\sigma^2_{W_k}$, which are related to the force intensity $F_{x(max)}$ and the time interval of Δt by:

$$\sigma^2_{W_k} = \frac{F_{x(max)}}{\Delta t} \tag{51}$$

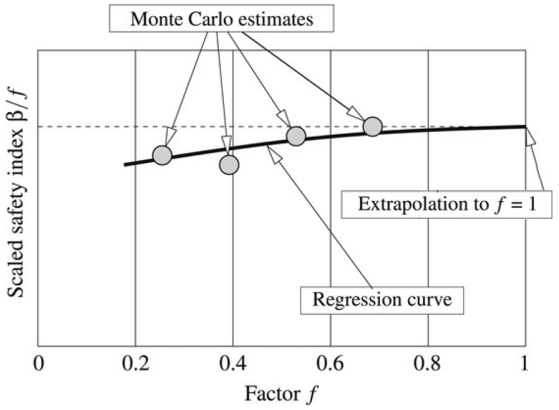

FIGURE 4. Asymptotic sampling method extrapolation process [1], [37].

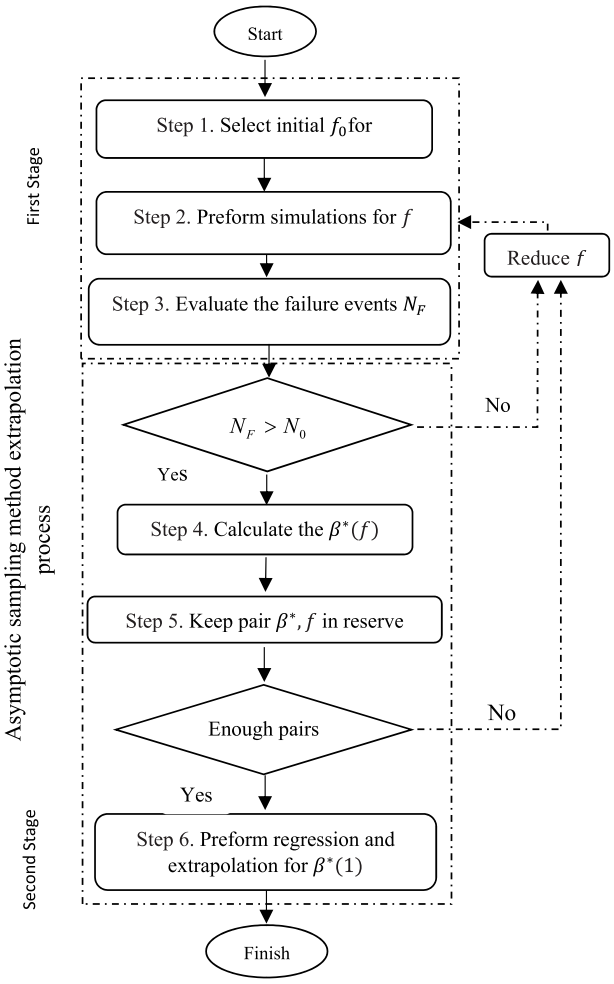

FIGURE 5. Fundamental flow-chart of asymptotic sampling method [1].

Subsequently, in order to apply the reliability analysis, it is considered that the braking force can be demonstrated by a sequence of IID. random variables U_k which have a unit standard deviation. Therefore, the variables W_k can be defined by:

$$W_k = \sqrt{\frac{F_{b(max)}}{\Delta t}} U_k \tag{52}$$

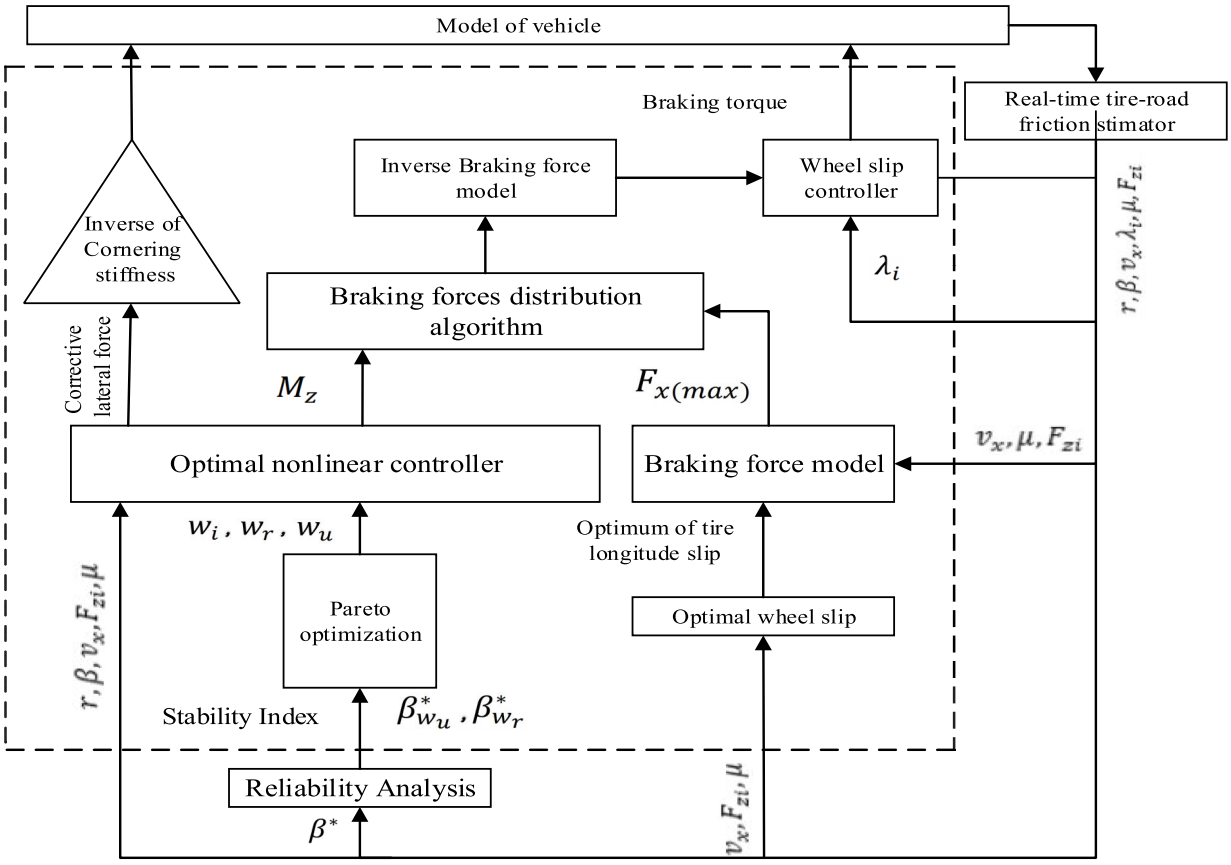

FIGURE 6. Overview of design, optimization, and control procedure of the system.

VII. SIMULATION AND ANALYSIS

The overview of the design, optimization, and control procedure of the proposed control system is shown in Figure 6. Here, the performance of the designed control system for the vehicle on the braking situation concerning to different strategies is simulated and analyzed. Road condition is considered to be a split-μ surface for all evaluations. The 5-DOF nonlinear vehicle model which has validated in the previous studies Smith and Starkey [78] is used to validate and compare the simulations. Therefore, the accuracy and the capability of the designed control system can be defined concerning the unstructured uncertainty in unmodelled dynamics. The discrepancy of the simulation model and each layer of controller design model can be leads to this uncertainty. Thus 5% uncertainty is presumed to be happen related to the structure, tire and vehicle parameters like as the tire stiffnesses (longitudinal and lateral) and the total mass and the yaw axis moment of inertia, respectively. Also, the same uncertainty can be considered for the possible inaccuracy in the assessment of the road coefficient of friction. In this research, the brake pressure actuator dynamics considered to be fast, and it is not assumed in the slip controller design (mentioned that the assumed uncertainty value is arbitrary).

In order to evaluate the vehicle stability control system based on the wheel slip control (both wheel slip and yaw moment control) with applying probabilistic design, the CarSim, Simulink and design of experiments joint software simulation are used. The braking manoeuvring on a split-road in the severe condition is proposed with road frictions of coefficient is 0.8 (wet asphalt) and 0.18 (snowy road). It is assumed that the vehicle speed in travelling is 120 km/h in the straight line, suddenly the vehicle needs to stop by hard braking. The road has a coefficient of friction 0.8 (wet asphalt) for both sides at the time braking is started. Simultaneously the right side of the road changes to the snowy road with the coefficient of friction 0.18, between 10m to 20m and again comes back to the 0.8 for the wet asphalt (left side has the constant coefficient of friction at 0.8 at all times). The expected goals are to decrease the braking distance with keeping in the straight line. The vehicle parameters are shown in Table 1.

A. ANALYSIS OF REAL-TIME TIRE-ROAD FRICTION CONDITIONS

In this paper, the estimation strategies are used and have tried to define the acceptable performance levels cornering to the braking application. Considering to the accuracy requirements which are dependent to the vehicle electronics and control devices characteristics, ±5% accuracy estimation assumed for the peak of the friction curve and is proper for

TABLE 1. Parameters of vehicle used for the simulation [85].

Description	Values and units
Mass of vehicle	1500 kg
coefficient of Aerodynamic drag	0.6
Half of the wheel base	0.75 m
Front wheel axle to CG distance	1.2 m
Rear wheel axle to CG distance	1.6 m
Yaw moment of inertia	3240 kg m^2
Lateral wheel base (Track width)	1.436
Distance from sprung mass cg to roll axis	0.45

ABS control as reported in [102]. Moreover, the information of estimator should be reliable concerning to time instant to use in the braking controller. Therefore, the parameters wheel speed (ω), vehicle speed (v_x) and braking torque T_b considered to be defined on noisy simulations and white noises have zero mean which have added. The estimations conducted with 20 samples with the maximum likelihood estimation approach (ML approach). The parameter assessment results by the ML approach is shown in Table 2.

TABLE 2. The $\mu(\lambda)$ estimation results based on ML simulation data on noisy simulation data.

		Road condition $\mu = 0.8096$	Road condition $\mu = 0.1887$
True values	ϑ_1	0.88	0.42
	ϑ_2	34.8	98.35
	ϑ_3	0.36	0.08
ML Estimation	$\hat{\vartheta}_1$	0.876	0.38
	$\hat{\vartheta}_2$	31.98	94.95
	$\hat{\vartheta}_3$	0.37	0.06

It should be noted that according to achieve good and accurate estimations of the unknown parameters, the ML estimator needs to update continuously. On this view, it can be presumed that the varying acceleration can give us efficient information for estimation. Therefore, a wide range of variation should be considered in the computer simulations by applying the slip controller for the input information of estimator to define a varying reference. Hence, the reference slip is decided to be 0.1 [Hz] as a sinusoidal signal concerning different simulations, different magnitudes are estimated. The sinusoidal slip reference magnitude varying from 0.005 to 0.4 during the simulations on the braking condition and results are summed up in Table 3 and Table 4. The averaged inputs are used in the repeated simulations. The estimated friction curves are presented in Figure 7(a) and (b). The friction curves are estimated after approximately 4 seconds of driving on snowy and wet asphalt roads. The actual friction curve achieved by the Burckhardt friction model has shown in Figure 7(a) and (b).

Concerning Figure 7(a) and (b), it is found that the good estimation of the initial slope μ for the friction curve has conducted and on the higher slip references, the curve estimation is more reliable. It should be noticed that defining good

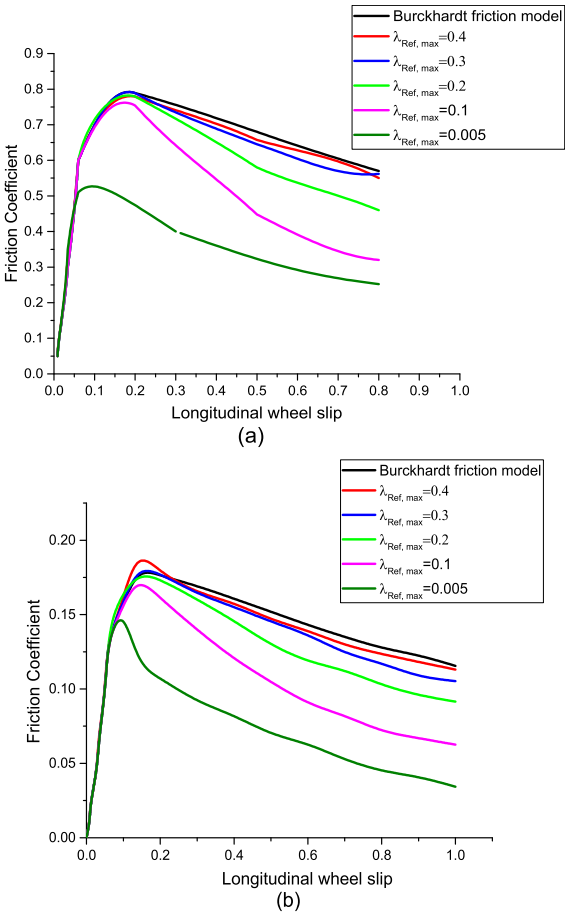

FIGURE 7. Friction curve estimations simulations for different slip reference magnitudes on: (a) wet asphalt, (b) on snow.

TABLE 3. The λ_{max} estimation performances results bases on ML simulation data on wet asphalt condition with true values of $\lambda_{max} = 0.1410$ and $\mu = 0.8096$.

		ML Estimation				
Road condition $\mu = 0.8096$ (Wet asphalt)		$\lambda_{\text{ref (max)}} = 0.005$	$\lambda_{\text{ref (max)}} = 0.1$	$\lambda_{\text{ref (max)}} = 0.2$	$\lambda_{\text{ref (max)}} = 0.3$	$\lambda_{\text{ref (max)}} = 0.4$
	$\hat{\lambda}_{max}$	0.0582	0.1398	0.1425	0.1431	0.1445
	$\hat{\mu}_{max}$	0.7583	0.7812	0.7994	0.8033	0.8094
	$\frac{\mu(\hat{\lambda}_{max})}{\mu(\lambda_{max})}$	0.93	0.96	-1.05%	0.987	0.99

estimation of the friction curve peak needed that the slip can gain values near λ_{max} (this is not considered for the lowest slip reference). Also, it can be seen that the friction curve has a low slope in the adjacency of the λ_{max} and indicate that a large part of the available friction can be considered whether the λ_{max} is not correctly estimated. Therefore, evaluating of the available friction amount in terms of stabilized slip at $\hat{\lambda}_{max}$ compared to λ_{max} is considered and λ_{max} estimations concerning to wet asphalt, snowy surfaces and magnitudes of slip reference are presented. The λ_{max} true value is also presented in Tables 3 and 4.

TABLE 4. The λ_{max} estimation performances result based on ML simulation data on snowy condition with true values of $\lambda_{max} = 0.0605$ and $\mu = 0.1887$.

		ML Estimation				
			$\lambda_{\text{ref (max)}} = 0.005$	$\lambda_{\text{ref (max)}} = 0.1$	$\lambda_{\text{ref (max)}} = 0.2$	$\lambda_{\text{ref (max)}} = 0.3$
Road condition $\mu = 0.1887$ (Snow)	$\hat{\lambda}_{max}$	0.038	0.0695	0.0779	0.0798	0.0828
	$\hat{\mu}_{max}$	0.1792	0.1799	0.1854	0.1866	0.1872
	$\frac{\mu(\hat{\lambda}_{max})}{\mu(\lambda_{max})}$	0.94	0.95	0.982	0.988	0.99

B. BRAKING CONTROL SIMULATIONS AND ASSESSMENT

In this section, simulations are conducted on the vehicle braking performance concerning with and without control systems. Therefore, the stand-alone braking control in different situations of direct yaw moment control ($\gamma = 0$, cheap control), without direct yaw moment control ($\gamma = \infty$, expensive control), integrated control (applying weighting ratio on the side slip and external yaw moment) and probability approach are simulated for controlled system. Finally, the probability approach results compared with the other control strategies to define the effeteness.

1) WITHOUT CONTROL STRATEGY

The driver has tried to stop the vehicle by hard braking and subsequently, all the wheels become locked. The braking forces of tires are shown in Figure 8. It can be seen that because of changes on the road friction coefficient on the braking path, a large contrast on the forces of tires on the left and right side has generated by braking (within 0.5 to 1 s) and leads to vehicle slide.

2) STAND-ALONE STRATEGY

The stand-alone strategy for braking control is conducted to regulate the vehicle motions at extreme amounts on the longitudinal and lateral directions. Concerning the control law Eq. (37) and the weighting ratio at limit conditions, cases (1) the braking control without direct yaw moment control ($\gamma = \infty$) and (2) fully used direct yaw moment control ($\gamma = 0$,) are discussed. At the first case, the maximum braking forces are used to decrease the braking distance to the minimum (conventional ABS). In the second case, the controller tried to remain the vehicle in the straight direction. Comparison of the right side braking forces of tires and the left side tires are shown in Figure 8. It can be seen that the difference of braking forces at maximum values in the right and left side tires have a significant effect on the vehicle controlling which the directional stability cannot improve at the conventional ABS ($\gamma = \infty$) as shown in Figure 8(b), but enhance the directional stability by applying proper distribution of braking forces in case $\gamma = 0$, as shown in Figure 8(c).

3) INTEGRATED STRATEGY

In the integrated control case, a compromise is tried to achieve between the vehicle deviation from the straight direction and the stopping distance by applying the control law Eq. (37) and conducting the weighting ratio γ. Therefore, the controller makes an effort to reduce the distance of stopping until the vehicle does not pass the admissible deviation limit. Thus, improvement of the directional stability can be possible by defining minimum possible values for the external yaw moment. This can be possible by concerning sufficient yaw rate near zero value, which resulted to minimum braking distance. Consequently, the weighting ratio γ increment leads to the reduction of yaw moment with respect to some acceptable tracking error for the yaw rate at zero value. Then, the necessary moments created by the distribution of braking forces transversely. Distribution of braking forces of the vehicle on the right and left side concerning different control strategies on the split-μ road are presented in Figure 8(d).

A better comparison of the controls system can be conducted by evaluating the Yaw rate, side-slip angle and

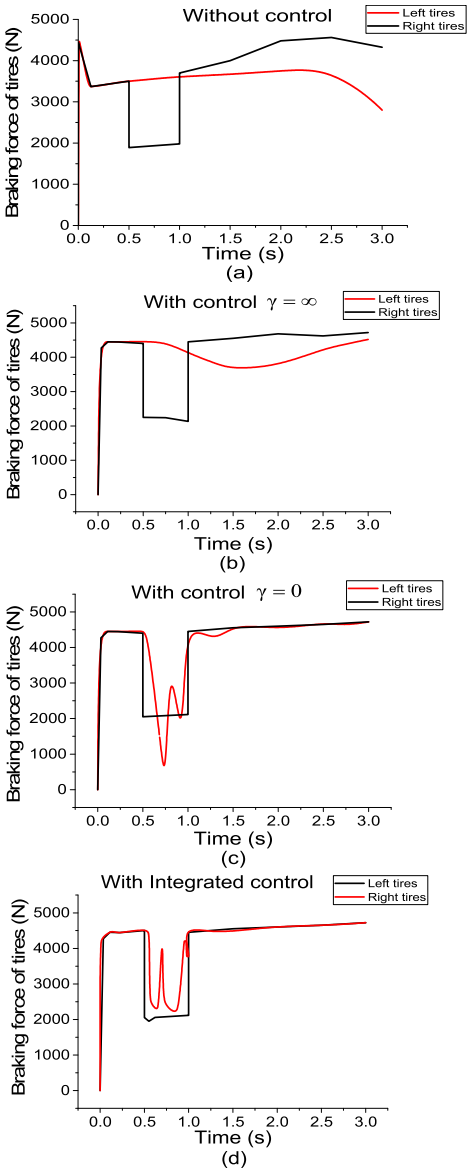

FIGURE 8. Comparison of the braking forces for four cases: (a) without control, (b) with control ($\gamma = \infty$, expensive control), (c) with ($\gamma = 0$, cheap control), (d) Integrated control.

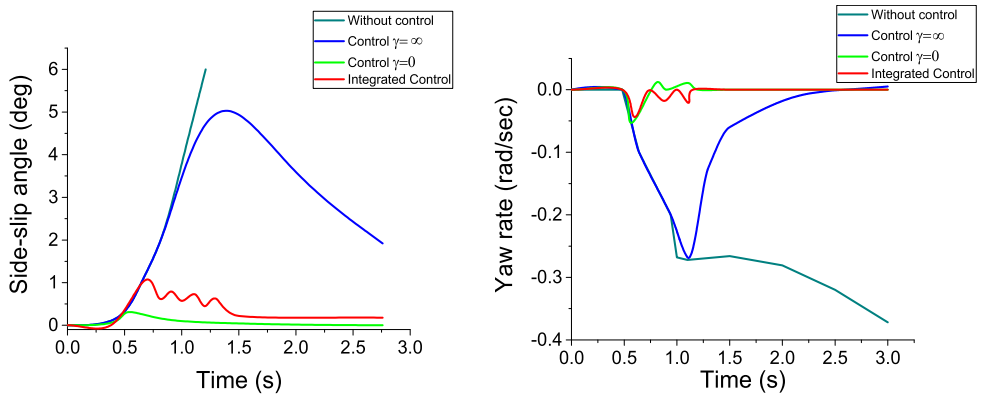

FIGURE 9. Comparison of the yaw rate and the side-slip angle for four cases: without control, with control ($\gamma = \infty$, expensive control), with ($\gamma = 0$, cheap control), Integrated control.

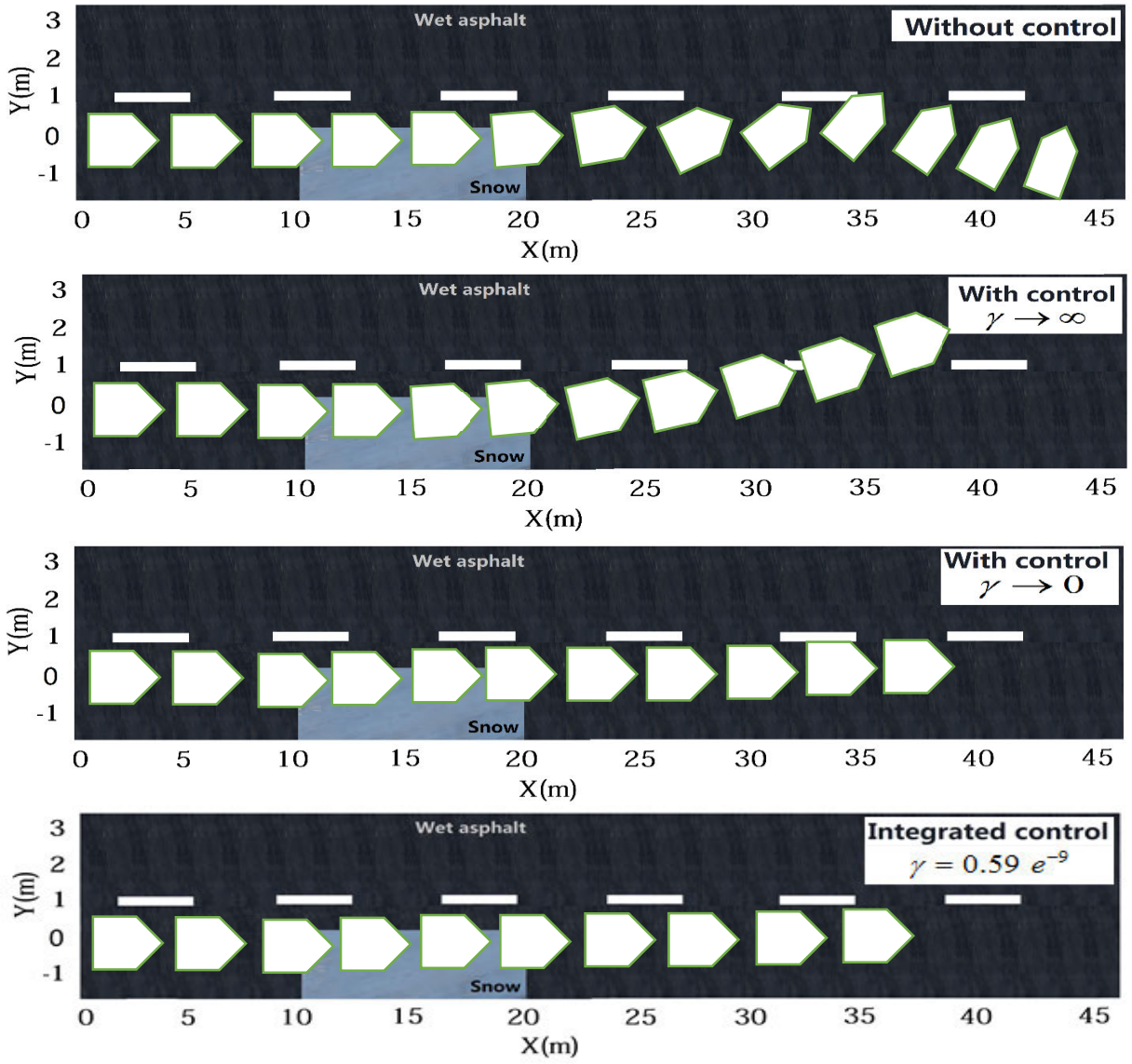

FIGURE 10. Comparison of the vehicle trajectory for four cases: (a) without control, (b) with control ($\gamma = \infty$, expensive control), (c) with ($\gamma = 0$, cheap control), (d) Integrated control.

external yaw moment. Hence, the side-slip angle and the yaw rate responses concerning the time dependency are evaluated in Figure 9(a) and (b). Also, the vehicle trajectories are figured out in Figure 10. As a consequence, an unanticipated

TABLE 5. Summary of weighting ratio γ assessment performance concerning to stopping distance and maximum directional deviation.

Weighting ratio on external yaw moment (γ)	Stopping distance (m)	maximum directional deviation (from the straight line (m))
0 (fully-used direct yaw moment control)	37.98	0.11
$\mathbf{0.21\ e^{-9}}$	37.64	0.28
$\mathbf{0.59\ e^{-9}}$	37.08	0.44
$\mathbf{1.19\ e^{-9}}$	36.95	0.61
$\mathbf{2.1\ e^{-9}}$	36.55	0.9
∞ (conventional ABS)	36.25	1.4

yaw moment in the without control case leads to deviation in the vehicle directional stability. The stand-alone case indicates that fully used direct yaw moment control ($\gamma = 0$) is control braking by the quickly tracking of the desired yaw rate value ($r_d = 0$) and try to maintain the angle of side-slip to be close to zero. The vehicle trajectory at $\gamma = 0$ shows an enhancement on the directional stability of vehicle which is conducted by the generation of proper external yaw moment in cost of a decrease in the maximum braking force on the one of vehicle sides. But unfortunately, a considerable increment in stopping distance has observed. Table 5 Shows the Stopping distance and maximum deviation of the vehicle for the limit values of the weighting ratio. On the other hand, minimum stopping distance can be defined by decreasing the external yaw moment value at the limit point. Hence, the weighting ratio γ (control law Eq. (37)) has increased, but it should be noted that the tracking error for the yaw rate at zero value is unavoidable. The stopping distance for the cases of $\gamma = 0$ and $\gamma = \infty$ are 37.98 m and 36.25 m, respectively. Also, the vehicle trajectories are confirmed the achieved outcomes (shown in Figure 10).

The case of integrated control conducted by trying to achieve a balance between the desirable values of stopping distance reduction and keeping the vehicle on the straight line. Therefore, weighting ratio has regulated concerning the limit values in the control law Eq. (37). The road margins width and location of the vehicle are considered to define permissible deviation range for the vehicle manoeuvring during braking. Therefore, by assuming 4 m road width, the maximum deviation of 0.45 m can be acceptable. Different values of the γ with respect to the stopping distance and deviation are presented in Table 5.

As a result, the value of $\gamma = 0.59e^{-9}$ leads to a more stable situation considering simulation conditions in the integrated control case which the minimum achieved stopping distance is 37.08 m and comparing with case $\gamma = 0$ the distance has shorter value is about 0.9m. The vehicle trajectory for this case is displayed in Figure 9 with enhancing on stopping distance and vehicle stability. Thus, as Table 5 demonstrated both dynamics on the longitudinal and lateral directions have a scientific effect on the vehicle stability concerning to control brake track and vehicle directional steering on hard braking with respect to the road condition.

Paying attention to Figure 9, it is indicated that the slip has well stabilized by the slip controller at the reference value in the integrated, cheap ($\gamma = 0$) and expensive ($\gamma = \infty$) control strategies. The slip has settled in 2 % of the reference in 1.5 s for the two control strategies (Integrated and cheap controls) which is slightly slower happened for the expensive control. Also, in the braking simulation, the vehicle velocities start to decrease by oscillatory increasing in the slip and yaw rate responses.

Accordingly, the control system dependency on the weighting ratio γ can be seen in Figure 9 and Figure 10, which increase of γ leads to a reduction of external yaw moment and as a consequence the yaw rate and directional deviation are increased. Besides, a reduction in stopping distance is due to the increase in the values of the weighting ratio (Table 5).

C. RELIABILITY CONTROL ANALYSIS

To monitor the vehicle braking stability by the reliability analysis, the main design requirements should be defined. Therefore the first-passage probabilities are applied to estimate the reliability indices for the weighting ratios quantities which are assumed as: (1) Maximum value of w_u and (2) Maximum value of w_r. These ratios are important to indicate the error and energy relation in the assessment of the performance index at minimum value concerning the external yaw moment and wheels corrective lateral forces. The analytical study is applied by the first-passage analysis and the threshold values are confined in $w_u = (5 \times 10^{-13})\hat{w}_u$ for the maximum control on the vehicle directional deviation and $w_r = (5 \times 10^{-12})\hat{w}_r$ for the minimum stop distance of the vehicle by using the braking forces of wheels at maximum value. It should be noted that $\beta^*_{w_u}$ and $\beta^*_{w_r}$ are the corresponding reliability indices and the above threshold values are adjusted through some trials.

The procedure of reliability braking simulation is discretized at the time interval $\Delta t = 0.005$ s for each braking and the total duration of 5s. From this aspect, it means that the braking process is illustrated by 1000 random variable simulations. Asymptotic sampling method (explained in reliability modelling) with five support points ($k = 5$) is used to define the first-passage probabilities. Each support points is based on 200 Monte Carlo samples. To describe more, system parameters variation causes wide variation in the first-passage probabilities. Therefore, the search method described in flow chart Figure 5 has been applied to define the factor f in an increasing way. The method automatically continued until five support points have been defined which have stable probability estimates.

In general, each reliability indices and each point (γ, M_z) in the design space need almost 1000 Monte Carlo samples. The uniformly distributed Latin Hypercube sampling method is used to cover the variation of braking force and the coefficient of friction (with respect to the time variation of coefficient friction) by using simulation design and using 100 sample points. The intervals chosen are $-500N.m \leq M_z \leq 2000N.m$

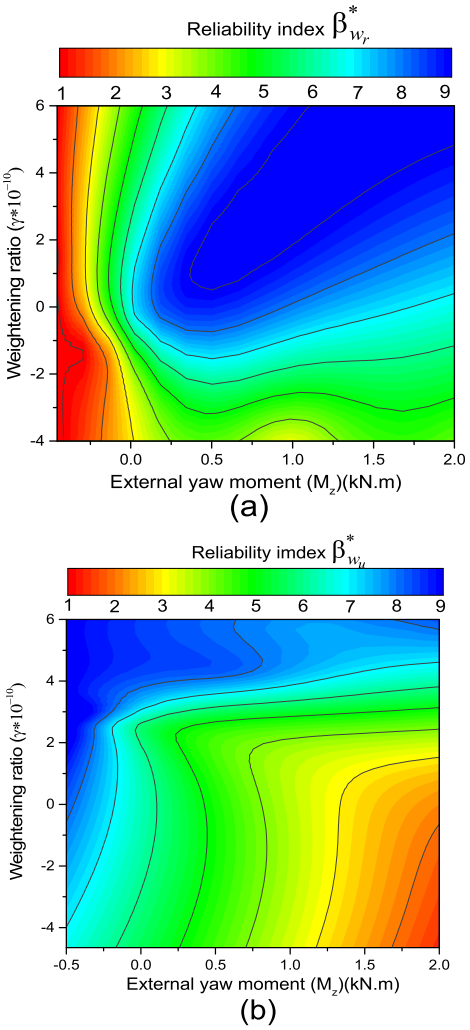

FIGURE 11. First-passage reliability β_{wu}* and $\beta^*_{w_r}$ indices of maximum performance depending on weighting ratio γ and external yaw moment M_z (MLS smoothing).

and the weighting ratio changes between zero and infinitive. The optimization process is involved $\beta^*_{w_u}$ and $\beta^*_{w_r}$ and conducting by dynamic analyses with about 300,000 runs. Each analysis run takes time for about 2s on a normal PC; thus about 166 h of computation time is needed totally.

First-passage reliability $\beta^*_{w_u}$ and $\beta^*_{w_r}$ maximum performance indices are determined by weighting ratio (γ) and external yaw moment (M_z) and represented in Figure 11. It should be noted that the calculated design spaces of $\beta^*_{w_u}$ and $\beta^*_{w_r}$ have a considerable fluctuation which comes from the lack of statistical certainty of reliability indices estimated by the Monte-Carlo method. Therefore, in order to eliminate the fluctuations, smoothing techniques [17], [29] which employ to improve the response surface methods is applied [103]. Here, the smoothing procedure has been conducted by the Moving Least Squares method [104]–[107]. The reliability index $\beta^*_{w_u}$ is smoothed with respect to the design space and has been shown in Figure 11(a). In order to keep the maximum directional deviation small, directional stability of the

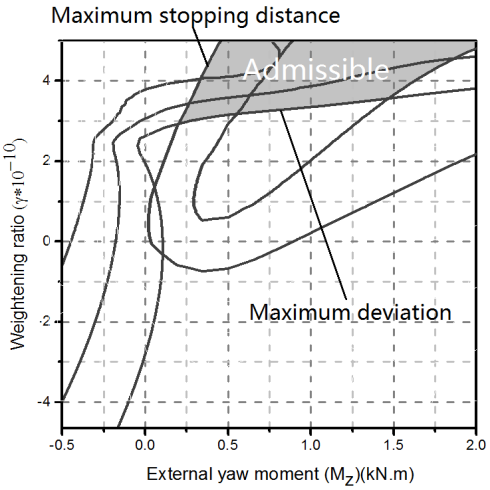

FIGURE 12. The admissible domain of weighting ratio γ and external yaw moment M_z for maximum performance problem.

vehicle is provided by external yaw moment. The braking force reduction is intentionally and applied to create the moment at external yaw direction and stopping the vehicle. Therefore a large external yaw moment M_z and a smaller w_u (small weighting ratio γ) is helpful.

The first-passage safety index $\beta^*_{w_r}$ for the maximum stopping distance depending on weighting ratio γ and external yaw moment M_z is shown in Figure 11(b). It can be seen that the primary variable to keep the maximum stopping distance small has the lower values of w_r (large weighting ratio γ). On the other hand, small values of w_r with reliability index $\beta^*_{w_r}$ decrease the braking distance by employing braking forces at maximum value to the wheels. Figure 11(a) and (b) are compared the reliability indices. It can be noticed that a small region of weighting ratio (γ) and external yaw moment (M_z) in total design space are overlapped with respect to reliability indices $\beta^*_{w_r}$ and $\beta^*_{w_u}$. This small region can be used to define appropriate large values of all β^*-values. Here, it is assumed that all safety indices are needed to have values larger than 7; thus the design space is reduced to the smaller part that indicated the admissible domain, as shown in Figure 12.

It can find out even though the admissible domain has been defined in design space, the indices of maximum performance based on first-passage probabilities demonstrate incompatible objectives with respect to weighting ratio and external yaw moment. Therefore, in order to improve the decision making, applying a Pareto type approach might be brought up.

Consider a multi-objective minimization problem. It has m scalar valued objective functions, which identify by $f_k : D_x \subset \mathbb{R}^n \Longrightarrow \mathbb{R}$. Then X* can be considered as a non-dominated value if [108]:

$$\begin{cases} f_k(\mathrm{X}^*) \leq f_k(X)\ \forall k \forall X \in D_x \\ \text{and} \\ \exists l : f_l(\mathrm{X}^*) < f_l(X)\ \forall X \in D_x \end{cases} \tag{53}$$

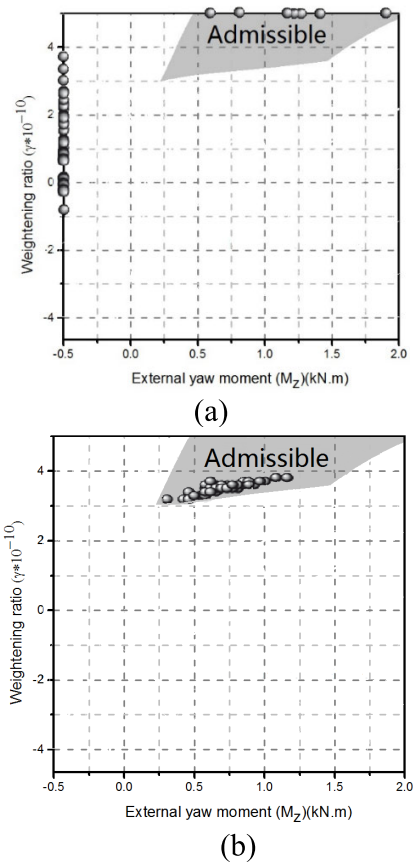

FIGURE 13. Pareto set points for multi-objective performance optimization problem: (a) reliability indices at maximum values, (b) probability-based performance optimization cost function at minimum setpoint values.

To define the solution set of all non-dominated equations for an m-objective problem, all the solutions X_α should be assembled concerning to the all cumulated optimization problems of the form:

$$f_\alpha = \sum_{k=1}^{m} \alpha_k f_k\,(X) \rightarrow Min. \tag{54}$$

where α_k have positive values of the coefficient which satisfying $\sum_{k=1}^{m} \alpha_k = 1$. The coefficients can be provided by considering u_k as the random numbers. u_k are uniformly distributed in the interval [0, 1] and normalized as:

$$\alpha_k = \frac{u_k}{\sum_{k=1}^{m} u_k} \tag{55}$$

Concerning that the calculation is performed by using the response surface, which has been provided by the MLS smoothing procedure, the calculation attempt can be ignored. On the other hand, if the number of problems is more, using the alternative method which using the evolutionary strategies [106], [108], [109], is more convenient. These approaches and their applications are illustrated profoundly in [110], [111]. Referred to the problem here, the objective functions are defined by applying the reliability indices directly, as shown in Figure 13(a). The Pareto set just composed of the boundary points of the design space, and it cannot be possible to reach a real agreement. In order to untangle this situation, the failure probabilities are applied instead of the reliability indices. Therefore, the aggregated objective function should be minimized as:

$$C = \alpha_1 \cdot \Phi\left(-\beta^*_{w_u}\right) + \alpha_2 \cdot \Phi\left(-\beta^*_{w_r}\right) \tag{56}$$

Applying the probabilities instead of the reliability indices conducted to an anticipated cost function including the possible consequences which are considering the possibility of failure in braking controller or parts of the controller too. Figure 13(b) shows the transparent compromise area are which is determined by the Pareto set.

Concerning Figure 13, it can be found that the external yaw moment is confined less by applying the multi-objective optimization than the weighing ratio in charge of the performance and stability of the braking system. Also, it can be seen that the probability area encompasses the admissible area with respect to all reliability indices with values larger than 7. The results for probability-based control strategy are shown in Table 6. In this region, the optimal weighting ratio of the order of $\gamma = 3.383e^{-10}$, and the optimal external yaw moment is about $M_z = 1.286e^2$. The Comparison of performance for different control strategies included the probability case has shown in Figure 14.

TABLE 6. Summary of performance assessment concerning to stopping distance and maximum directional deviation for probability-based control strategy.

Analysis model	Weighting ratio on external yaw moment (γ)	external yaw moment (M_z)	Stopping distance (m)	Maximum directional deviation (from the straight line (m))
Probability model	3.83 e^{-10}	1.286 e^2	36.19	0.121

The probability control strategy results are compared with other strategies in Figure 14. As can be found from performance graphs in Figure 14 (a), (b) and (c), meanwhile the stopping distance is reduced by adjusting zero yaw rate and confining the side-slip angle at the same instant, the braking control is applied for integrating the steering control to deduct the external yaw moment contribution. Also, it can be seen that in the probability, integrated and fully-used direct yaw moment ($\lambda = 0$) control strategies, the zero yaw rate is closely adjusted.

It should be noted that in the probability and integrated control strategies, the possible responses domain is small and as a consequence, the vehicle directional stability and stopping performance is enhanced. However, the contribution of external yaw moment in the probability strategy is remarkably decreased. Although there is a considerable reduction in the contribution of the external yaw moment in the probability strategy (Figure 14 (c) and (d)), this considerable reduction is conducted by the optimal probability base optimization of the steering and braking control. So, the shorter stopping distance

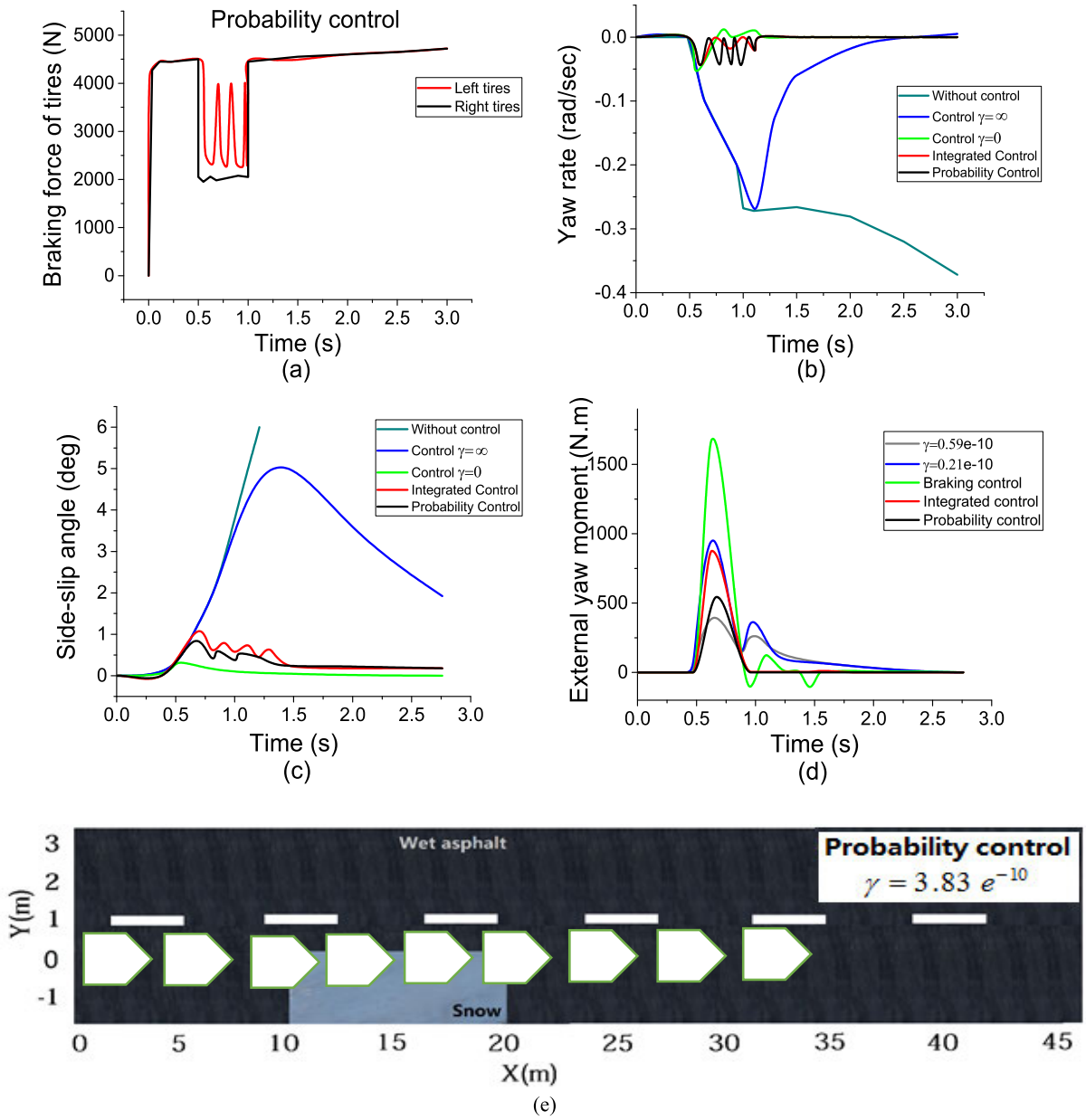

FIGURE 14. Performance comparison of different control strategies: (a) braking force of tires (reliability case), (b) yaw rate (all cases), (c) the side-slip angle (all cases), (d) external yaw moment (all cases), (e) vehicle trajectory (reliability case).

can be achieved due to the less decrease in the braking forces at maximum value.

The probability control strategy enhanced the stopping distance and it has decreased about 0.89m in comparison with the braking with an integrated control strategy. Simultaneously, a considerable reduction can be seen in the vehicle directional deviation Figure 14(e) (the vehicle trajectory). The weighting ratio of control input (γ) determined from the ''admissible'' area which Pareto multi-objective optimization is depicted in Figure13(b). The importance of control inputs can be explained by the relative effect on the decrease or increase of the weights to each other. In this way, the vehicle performance in hard braking enhances while the weights of external yaw moment (w_u) are decreased and simultaneously the corrective lateral forces of the wheels (w_r) are increased.

VIII. CONCLUSIONS

A probabilistic basis control system for vehicle braking and directional stability concerning to the optimal design on the nonlinear algorithm for appropriate tire braking forces distribution and external moments is presented. The main purpose of this controller is to enhance the braking performance by adjusting the maximum value of braking forces of the vehicle wheels as low as possible and subsequently generate the minimum stabilizing yaw moment. The nonlinear vehicle responses are predicted and are applied to develop the control

laws in different layers of analysis. Two control inputs are considered, and the optimal weights of the control law are tried to define. Therefore, the objective functions in the whole design space of the input variables weighting ratio (γ) and external yaw moment (M_z) are demonstrated by a Moving Least squares response surface based on a Latin Hypercube design of experiments. Concerning the design parameters of the braking control, an enormous number of computations needed to define the probabilities of failure. Therefore to tackle and manage the computing process, an efficient technique based on Monte-Carlo simulation which is called asymptotic sampling has been employed.

The braking system controller system has been utilized by a Pareto-type optimization approach. A cost function including the first-passage probabilities of the maximum distance of stopping and maximum directional deviation has applied to formulate the objectives with respect to the external yaw moment and the wheel corrective lateral forces. Therefore, applying this method has enabled to perform the calculation of reliability problems with the high-dimensionality by conducting a small number of limit state assessments (about several hundred). Also, this approach gives a considerable privilege of non-dimensionality of its outcomes and efficacy. It has been demonstrated that the very low braking failure probability ($\beta^* = 7$) consisting up to 10^5 random variables have a possibility to be conducted with a small sample size of simulation (10^3 samples) with appropriate precision. Therefore, the objective functions have carried out with a reliable presence in the whole design space.

As a main final outcome, the control law parameters in optimal condition has been restricted in a comparatively tight and narrow range. Consequently, a compromise on the derived range of the directional deviation and stopping distance has conducted. The simulation results have indicated that the presented probability-based control system has enhanced directional stability. It has resulted in the shorter stopping distance (about 0.89m) and improves about 70% steering performance during the hard braking (0.09m deviation from the straight line) in comparison with the other braking control system.

APPENDIX
FRICTION BETWEEN TIRE AND ROAD REAL TIME IDENTIFICATION STRATEGY

Estimation of $\mu(\lambda)$ can be possible by set up a curve fitting based problem; subsequently λ_{max} is defined by the estimated results based by friction fitted curves. Therefore, a standard quadratic error function at minimum values is applied as:

$$J(\vartheta) = \frac{1}{N}\sum_{i=1}^{N} \varepsilon(\lambda_i, \vartheta)^2 \tag{A-1}$$

where samples number represented by the N and $\varepsilon(\lambda_i, \vartheta)$ defined the error of estimation as:

$$\varepsilon(\lambda_i, \vartheta) = \mu(\lambda_i) - \hat{\mu}(\lambda_i, \vartheta) \tag{A-2}$$

Subsequently in order to do fitting process on the tire-road friction curve the Maximum Likelihood Approach is used [112], [113]. Using a quasi-Newton method with an iterative minimization technique is conducted to indicate the error fitting with respect to the Eq. (30) [112], [113]. The method using each iteration to adjust the vector's parameters based on:

$$\vartheta^{(r+1)} = \vartheta^{(r)} + \left(\sum_{i=1}^{N} \xi(\lambda_i)\xi(\lambda_i)^T\right)^{-1} \left(\sum_{i=1}^{N} \xi(\lambda_i)\varepsilon(\lambda_i)\right) \tag{A-3}$$

where

$$\xi(\lambda_i) = -\frac{\mathrm{d}\varepsilon(\lambda_i)^T}{\mathrm{d}\vartheta}\left[1 - e^{-\lambda_i\vartheta_{r2}}\vartheta_{r1}\lambda_i e^{-\lambda_i\vartheta_{r2}} - \lambda_i\right]^T \tag{A-4}$$

It should be noted that An ad hoc empirical approach is used to initialize the vector's parameter which is the decisive step in the ML approach. Practically, Burckhardt model is used to approximate the wheel slip low values as:

$$\mu(\lambda, \vartheta_r) \cong (\vartheta_{r1}\vartheta_{r2} - \vartheta_{r3})\lambda - \vartheta_{r1}\vartheta_{r2}^2\lambda^2 \tag{A-5}$$

Considering the very small range of variation in the parameter ϑ_{r3}, an average value can be consider as initial value for parameter $\hat{\vartheta}_{r3}(0)$. Afterwards, the initial values $\hat{\vartheta}_{r1}(0)$ and $\hat{\vartheta}_{r2}(0)$ can be define by using quadratic approximation on corresponded first initial available data to low slip values.

REFERENCES

[1] C. Bucher, "Asymptotic sampling for high-dimensional reliability analysis," *Probabilistic Eng. Mech.*, vol. 24, no. 4, pp. 504–510, Oct. 2009.

[2] M. T. Sichani, S. R. K. Nielsen, and C. Bucher, "Efficient estimation of first passage probability of high-dimensional nonlinear systems," *Probabilistic Eng. Mech.*, vol. 26, no. 4, pp. 539–549, Oct. 2011.

[3] F. Zareian and H. Krawinkler, "Assessment of probability of collapse and design for collapse safety," *Earthq. Eng. Struct. Dyn.*, vol. 36, no. 13, pp. 1901–1914, 2007.

[4] Y. Dong and D. M. Frangopol, "Probabilistic ship collision risk and sustainability assessment considering risk attitudes," *Struct. Saf.*, vol. 53, pp. 75–84, Mar. 2015.

[5] D. R. Karanki, H. S. Kushwaha, A. K. Verma, and S. Ajit, "Uncertainty analysis based on probability bounds (P-box) approach in probabilistic safety assessment," *Risk Anal.*, vol. 29, no. 5, pp. 662–675, May 2009.

[6] G. Apostolakis, "The concept of probability in safety assessments of technological systems," *Science*, vol. 250, no. 4986, pp. 1359–1364, Dec. 1990.

[7] G. W. Parry, "On the meaning of probability in probabilistic safety assessment," *Rel. Eng. Syst. Saf.*, vol. 23, no. 4, pp. 309–314, 1988.

[8] R. Ouache and M. N. Kabir, "Models of probability of failure on demand for safety instrumented system using atmospheric elements," *Saf. Sci.*, vol. 87, pp. 38–46, Aug. 2016.

[9] M. G. Stewart, D. V. Rosowsky, and D. V. Val, "Reliability-based bridge assessment using risk-ranking decision analysis," *Struct. Saf.*, vol. 23, no. 4, pp. 397–405, Oct. 2001.

[10] T. Aven and G. Reniers, "How to define and interpret a probability in a risk and safety setting," *Saf. Sci.*, vol. 51, no. 1, pp. 223–231, Jan. 2013.

[11] R. A. Howard, "Uncertainty about probability: A decision analysis perspective," *Risk Anal.*, vol. 8, no. 1, pp. 91–98, Mar. 1988.

[12] C. B. Brown and D. G. Elms, "Engineering decisions: Information, knowledge and understanding," *Struct. Saf.*, vol. 52, pp. 66–77, Jan. 2015.

[13] D. S. Dimitrova, V. K. Kaishev, and S. Zhao, "Modeling finite-time failure probabilities in risk analysis applications," *Risk Anal.*, vol. 35, no. 10, pp. 1919–1939, Oct. 2015.

[14] M. Forghani, J. M. McNew, D. Hoehener, and D. Del Vecchio, "Design of driver-assist systems under probabilistic safety specifications near stop signs," *IEEE Trans. Autom. Sci. Eng.*, vol. 13, no. 1, pp. 43–53, Jan. 2016.

[15] X. Yu, Q. Jia, M. M. Rashidi, and Z. Yang, "Comprehensive investigating on the aerodynamic influences of the wheel contact patch," *J. Appl. Comput. Mech.*, vol. 6, no. 4, pp. 934–955, 2019.
[16] S. Kim and D. M. Frangopol, "Decision making for probabilistic fatigue inspection planning based on multi-objective optimization," *Int. J. Fatigue*, vol. 111, pp. 356–368, Jun. 2018.
[17] C. Bucher and D. M. Frangopol, "Optimization of lifetime maintenance strategies for deteriorating structures considering probabilities of violating safety, condition, and cost thresholds," *Probabilistic Eng. Mech.*, vol. 21, no. 1, pp. 1–8, Jan. 2006.
[18] B. Xia, H. Lü, D. Yu, and C. Jiang, "Reliability-based design optimization of structural systems under hybrid probabilistic and interval model," *Comput. Struct.*, vol. 160, pp. 126–134, Nov. 2015.
[19] H. Lü, W.-B. Shangguan, and D. Yu, "A unified method and its application to brake instability analysis involving different types of epistemic uncertainties," *Appl. Math. Model.*, vol. 56, pp. 158–171, Apr. 2018.
[20] P. N. Ngatchou, A. Zarei, W. L. J. Fox, and M. A. El-Sharkawi, "Pareto multiobjective optimization," in *Proc. 13th Int. Conf., Intell. Syst. Appl. Power Syst.*, Arlington, VA, USA, 2007, pp. 189–207.
[21] C. Bucher, "Structural optimization under random dynamic seismic excitation," in *Encyclopedia of Earthquake Engineering*, M. Beer, I. A. Kougioumtzoglou, E. Patelli, S.-K. Au, Eds. Berlin, Germany: Springer, 2015, pp. 3617–3626.
[22] D. Straub, "Value of information analysis with structural reliability methods," *Struct. Saf.*, vol. 49, pp. 75–85, Jul. 2014.
[23] J. L. Chapman, L. Lu, and C. M. Anderson-Cook, "Process optimization for multiple responses utilizing the Pareto front approach," *Qual. Eng.*, vol. 26, no. 3, pp. 253–268, Jul. 2014.
[24] E. Zitzler and L. Thiele, "Multiobjective evolutionary algorithms: A comparative case study and the strength Pareto approach," *IEEE Trans. Evol. Comput.*, vol. 3, no. 4, pp. 257–271, Nov. 1999.
[25] A. Farhang-Mehr and S. Azarm, "Diversity assessment of Pareto optimal solution sets: An entropy approach," in *Proc. Congr. Evol. Comput. (CEC)*, 2002, pp. 723–728.
[26] C. A. Mattson and A. Messac, "Pareto frontier based concept selection under uncertainty, with visualization," *Optim. Eng.*, vol. 6, no. 1, pp. 85–115, Mar. 2005.
[27] A. M. Mirzendehdel and K. Suresh, "A Pareto-optimal approach to multimaterial topology optimization," *J. Mech. Design*, vol. 137, no. 10, pp. 101701-1–101701-12, Oct. 2015.
[28] H. A. Abbass, R. Sarker, and C. Newton, "PDE: A Pareto-frontier differential evolution approach for multi-objective optimization problems," in *Proc. Congr. Evol. Comput.*, 2001, pp. 971–978.
[29] H. Ackermann, A. Newman, H. Röglin, and B. Vöcking, "Decision-making based on approximate and smoothed Pareto curves," *Theor. Comput. Sci.*, vol. 378, no. 3, pp. 253–270, Jun. 2007.
[30] D. Sen and B. Bhattacharya, "On the Pareto optimality of variance reduction simulation techniques in structural reliability," *Struct. Saf.*, vol. 53, pp. 57–74, Mar. 2015.
[31] R. Gerrard and A. Tsanakas, "Failure probability under parameter uncertainty," *Risk Anal.*, vol. 31, no. 5, pp. 727–744, May 2011.
[32] A. Messac, A. Ismail-Yahaya, and C. A. Mattson, "The normalized normal constraint method for generating the Pareto frontier," *Struct. Multidisciplinary Optim.*, vol. 25, no. 2, pp. 86–98, Jul. 2003.
[33] I. Y. Kim and O. L. de Weck, "Adaptive weighted-sum method for bi-objective optimization: Pareto front generation," *Struct. Multidisciplinary Optim.*, vol. 29, no. 2, pp. 149–158, Feb. 2005.
[34] J. S. Sadowsky and J. A. Bucklew, "On large deviations theory and asymptotically efficient Monte Carlo estimation," *IEEE Trans. Inf. Theory*, vol. 36, no. 3, pp. 579–588, May 1990.
[35] C. J. Geyer, "Practical Markov chain Monte Carlo," *Stat. Sci.*, vol. 7, no. 4, pp. 473–483, Nov. 1992.
[36] K.-H. Jockel, "Finite sample properties and asymptotic efficiency of Monte Carlo tests," *Ann. Statist.*, vol. 14, no. 1, pp. 336–347, Mar. 1986.
[37] C. G. Bucher and U. Bourgund, "A fast and efficient response surface approach for structural reliability problems," *Struct. Saf.*, vol. 7, no. 1, pp. 57–66, Jan. 1990.
[38] M. Macke and C. Bucher, "Importance sampling for randomly excited dynamical systems," *J. Sound Vib.*, vol. 268, no. 2, pp. 269–290, Nov. 2003.
[39] A. Jamali, A. Hajiloo, and N. Nariman-Zadeh, "Reliability-based robust Pareto design of linear state feedback controllers using a multi-objective uniform-diversity genetic algorithm (MUGA)," *Expert Syst. Appl.*, vol. 37, no. 1, pp. 401–413, Jan. 2010.
[40] M. Macke and S. Higuchi, "Optimizing maintenance interventions for deteriorating structures using cost-benefit criteria," *J. Struct. Eng.*, vol. 133, no. 7, pp. 925–934, 2007.
[41] H. Zhao, "A multi-objective genetic programming approach to developing Pareto optimal decision trees," *Decis. Support Syst.*, vol. 43, no. 3, pp. 809–826, Apr. 2007.
[42] X. Hu, J. Jiang, B. Egardt, and D. Cao, "Advanced power-source integration in hybrid electric vehicles: Multicriteria optimization approach," *IEEE Trans. Ind. Electron.*, vol. 62, no. 12, pp. 7847–7858, Dec. 2015.
[43] N. Nariman-Zadeh, M. Salehpour, A. Jamali, and E. Haghgoo, "Pareto optimization of a five-degree of freedom vehicle vibration model using a multi-objective uniform-diversity genetic algorithm (MUGA)," *Eng. Appl. Artif. Intell.*, vol. 23, no. 4, pp. 543–551, Jun. 2010.
[44] J.-Y. Lee, M.-S. Kim, and J.-J. Lee, "Design of fuzzy controller for car parking problem using evolutionary multi-objective optimization approach," in *Proc. IEEE Int. Symp. Ind. Electron.*, Jul. 2006, pp. 329–334.
[45] M. Baum, J. Dibbelt, L. Hübschle-Schneider, T. Pajor, and D. Wagner, "Speed-consumption tradeoff for electric vehicle route planning," in *Proc. 14th Workshop Algorithmic Approaches Transp. Modelling, Optim., Syst.*, 2014, pp. 138–151.
[46] A. Jamali, M. Salehpour, and N. Nariman-Zadeh, "Robust Pareto active suspension design for vehicle vibration model with probabilistic uncertain parameters," *Multibody Syst. Dyn.*, vol. 30, no. 3, pp. 265–285, Oct. 2013.
[47] E. M. Kasprzak and K. E. Lewis, "An approach to facilitate decision tradeoffs in Pareto solution sets," *J. Eng. Valuation Cost Anal.*, vol. 3, no. 1, pp. 173–187, 2000.
[48] E. Hashemi, S. Khosravani, A. Khajepour, A. Kasaiezadeh, S.-K. Chen, and B. Litkouhi, "Longitudinal vehicle state estimation using nonlinear and parameter-varying observers," *Mechatronics*, vol. 43, pp. 28–39, May 2017.
[49] S. Ding, L. Liu, and W. X. Zheng, "Sliding mode direct yaw-moment control design for in-wheel electric vehicles," *IEEE Trans. Ind. Electron.*, vol. 64, no. 8, pp. 6752–6762, Aug. 2017.
[50] J.-S. Hu, Y. Wang, H. Fujimoto, and Y. Hori, "Robust yaw stability control for in-wheel motor electric vehicles," *IEEE/ASME Trans. Mechatronics*, vol. 22, no. 3, pp. 1360–1370, Jun. 2017.
[51] J. Cai, H. Jiang, L. Chen, J. Liu, Y. Cai, and J. Wang, "Implementation and development of a trajectory tracking control system for intelligent vehicle," *J. Intell. Robotic Syst.*, vol. 94, no. 1, pp. 251–264, Apr. 2019.
[52] J. J. Sinou, F. Thouverez, and L. Jézéquel, "Methods to reduce non-linear mechanical systems for instability computation," *Arch. Comput. Methods Eng.*, vol. 11, no. 3, pp. 257–344, Sep. 2004.
[53] H. Mirzaeinejad, M. Mirzaei, and R. Kazemi, "Enhancement of vehicle braking performance on split-μ roads using optimal integrated control of steering and braking systems," *Proc. Inst. Mech. Eng. K, J. Multi-body Dyn.*, vol. 230, no. 4, pp. 401–415, Dec. 2016.
[54] M. Kang, L. Li, H. Li, J. Song, and Z. Han, "Coordinated vehicle traction control based on engine torque and brake pressure under complicated road conditions," *Vehicle Syst. Dyn.*, vol. 50, no. 9, pp. 1473–1494, Sep. 2012.
[55] V. Ivanov, D. Savitski, and B. Shyrokau, "A survey of traction control and antilock braking systems of full electric vehicles with individually controlled electric motors," *IEEE Trans. Veh. Technol.*, vol. 64, no. 9, pp. 3878–3896, Sep. 2015.
[56] B. Wang, X. Huang, J. Wang, X. Guo, and X. Zhu, "A robust wheel slip ratio control design combining hydraulic and regenerative braking systems for in-wheel-motors-driven electric vehicles," *J. Franklin Inst.*, vol. 352, no. 2, pp. 577–602, Feb. 2015.
[57] T. Chen, L. Chen, X. Xu, Y. Cai, H. Jiang, and X. Sun, "Passive fault-tolerant path following control of autonomous distributed drive electric vehicle considering steering system fault," *Mech. Syst. Signal Process.*, vol. 123, pp. 298–315, May 2019.
[58] M. M. Rashidi, A. Hajipour, T. Li, Z. Yang, and Q. Li, "A review of recent studies on simulations for flow around high-speed trains," *J. Appl. Comput. Mech.*, vol. 5, no. 2, pp. 311–333, 2019.
[59] L. Li, X. Li, X. Wang, Y. Liu, J. Song, and X. Ran, "Transient switching control strategy from regenerative braking to anti-lock braking with a semi-brake-by-wire system," *Vehicle Syst. Dyn.*, vol. 54, no. 2, pp. 231–257, Feb. 2016.
[60] M. R. A. Atia, S. A. Haggag, and A. M. M. Kamal, "Enhanced electromechanical Brake-by-Wire system using sliding mode controller," *J. Dyn. Syst., Meas., Control*, vol. 138, no. 4, pp. 041003–6, Apr. 2016.

[61] J. J. Castillo, J. A. Cabrera, A. J. Guerra, and A. Simón, "A novel electrohydraulic brake system with tire–road friction estimation and continuous brake pressure control," *IEEE Trans. Ind. Electron.*, vol. 63, no. 3, pp. 1863–1875, Mar. 2016.

[62] C. M. Martinez, E. Velenis, D. Tavernini, B. Gao, and M. Wellers, "Modelling and estimation of friction brake torque for a brake by wire system," in *Proc. IEEE Int. Electric Vehicle Conf. (IEVC)*, Dec. 2014, pp. 1–7.

[63] P. Sinha, "Architectural design and reliability analysis of a fail-operational brake-by-wire system from ISO 26262 perspectives," *Rel. Eng. Syst. Saf.*, vol. 96, no. 10, pp. 1349–1359, Oct. 2011.

[64] L. Chen, T. Chen, X. Xu, Y. Cai, H. Jiang, and X. Sun, "Multi-objective coordination control strategy of distributed drive electric vehicle by orientated tire force distribution method," *IEEE Access*, vol. 6, pp. 69559–69574, 2018.

[65] M. Doumiati, O. Sename, L. Dugard, J.-J. Martinez-Molina, P. Gaspar, and Z. Szabo, "Integrated vehicle dynamics control via coordination of active front steering and rear braking," *Eur. J. Control*, vol. 19, no. 2, pp. 121–143, Mar. 2013.

[66] T. Hsiao, "Robust wheel torque control for traction/braking force tracking under combined longitudinal and lateral motion," *IEEE Trans. Intell. Transp. Syst.*, vol. 16, no. 3, pp. 1335–1347, Jun. 2015.

[67] S. Di Cairano, H. E. Tseng, D. Bernardini, and A. Bemporad, "Vehicle yaw stability control by coordinated active front steering and differential braking in the tire sideslip angles domain," *IEEE Trans. Control Syst. Technol.*, vol. 21, no. 4, pp. 1236–1248, Jul. 2013.

[68] H. Winner, S. Hakuli, F. Lotz, and C. Singer, *Handbook of Driver Assistance Systems: Basic Information, Components and Systems for Active Safety and Comfort*. Cham, Switzerland: Springer, 2016.

[69] J. Song, H. Kim, and K. Boo, "A study on an anti-lock braking system controller and rear-wheel controller to enhance vehicle lateral stability," *Proc. Inst. Mech. Eng. D, J. Automobile Eng.*, vol. 221, no. 7, pp. 777–787, Jul. 2007.

[70] R. Kazemi, B. Hamedi, and B. Javadi, "A new sliding mode controller for four-wheel anti-lock braking system (ABS)," SAE Technical Paper 2000-01-1639, 2000.

[71] J. Choby, "Systems and methods for determining road mu and drive force," Google Patents, Apr. 27, 2014.

[72] V. Ivanov, D. Savitski, K. Augsburg, P. Barber, B. Knauder, and J. Zehetner, "Wheel slip control for all-wheel drive electric vehicle with compensation of road disturbances," *J. Terramech.*, vol. 61, pp. 1–10, Oct. 2015.

[73] M. S. Basrah, E. Siampis, E. Velenis, D. Cao, and S. Longo, "Wheel slip control with torque blending using linear and nonlinear model predictive control," *Vehicle Syst. Dyn.*, vol. 55, no. 11, pp. 1665–1685, Nov. 2017.

[74] R. G. Hebden, C. Edwards, and S. K. Spurgeon, "Automotive steering control in a split-μ manoeuvre using an observer-based sliding mode controller," *Vehicle Syst. Dyn.*, vol. 41, no. 3, pp. 181–202, Jan. 2004.

[75] C. Ahn, B. Kim, and M. Lee, "Modeling and control of an anti-lock brake and steering system for cooperative control on split-μ surfaces," *Int. J. Automot. Technol.*, vol. 13, no. 4, pp. 571–581, Jun. 2012.

[76] M. S. Bang, S. H. Lee, C. S. Han, D. B. Maciuca, and J. K. Hedrick, "Performance enhancement of a sliding mode wheel slip controller by the yaw moment control," *Proc. Inst. Mech. Eng. D, J. Automobile Eng.*, vol. 215, no. 4, pp. 455–468, Apr. 2001.

[77] K. B. Singh and S. Taheri, "Estimation of tire–road friction coefficient and its application in chassis control systems," *Syst. Sci. Control Eng.*, vol. 3, no. 1, pp. 39–61, Jan. 2015.

[78] D. E. Smith and J. M. Starkey, "Effects of model complexity on the performance of automated vehicle steering controllers: Model development, validation and comparison," *Int. J. Vehicle Mech. Mobility*, vol. 24, no. 2, pp. 163–181, 1995.

[79] R. Wang, C. Hu, Z. Wang, F. Yan, and N. Chen, "Integrated optimal dynamics control of 4WD4WS electric ground vehicle with tire-road frictional coefficient estimation," *Mech. Syst. Signal Process.*, vols. 60–61, pp. 727–741, Aug. 2015.

[80] A. Karamoozian, C. A. Tan, and L. Wang, "Squeal analysis of thin-walled lattice brake disc structure," *Mater. Design*, vol. 149, pp. 1–14, Jul. 2018.

[81] A. Karamoozian, C. A. Tan, and L. Wang, "Homogenized modeling and micromechanics analysis of thin-walled lattice plate structures for brake discs," *J. Sandwich Struct. Mater.*, vol. 22, no. 2, pp. 423–460, Feb. 2020.

[82] M. Mirzaei and H. Mirzaeinejad, "Optimal design of a non-linear controller for anti-lock braking system," *Transp. Res. C, Emerg. Technol.*, vol. 24, pp. 19–35, Oct. 2012.

[83] H. Mirzaeinejad and M. Mirzaei, "A novel method for non-linear control of wheel slip in anti-lock braking systems," *Control Eng. Pract.*, vol. 18, no. 8, pp. 918–926, Aug. 2010.

[84] H. Mirzaeinejad and M. Mirzaei, "Optimization of nonlinear control strategy for anti-lock braking system with improvement of vehicle directional stability on split-μ roads," *Transp. Res. C, Emerg. Technol.*, vol. 46, pp. 1–15, Sep. 2014.

[85] S. M. Savaresi and M. Tanelli, "Introduction to active braking control systems," in *Active Braking Control Systems Design for Vehicles*. London, U.K.: Springer, 2010, pp. 3–16.

[86] J. Xu and D.-C. Feng, "Stochastic dynamic response analysis and reliability assessment of non-linear structures under fully non-stationary ground motions," *Struct. Saf.*, vol. 79, pp. 94–106, Jul. 2019.

[87] H. Koo, A. D. Kiureghian, and K. Fujimura, "Design-point excitation for non-linear random vibrations," *Probabilistic Eng. Mech.*, vol. 20, no. 2, pp. 136–147, Apr. 2005.

[88] S. L. Ho, S. Yang, G. Ni, E. W. C. Lo, and H. C. Wong, "A particle swarm optimization-based method for multiobjective design optimizations," *IEEE Trans. Magn.*, vol. 41, no. 5, pp. 1756–1759, May 2005.

[89] R. M. Bennett, "Structural analysis methods for system reliability," *Struct. Saf.*, vol. 7, nos. 2–4, pp. 109–114, Mar. 1990.

[90] M. H. Faber, *Statistics and Probability Theory: In Pursuit of Engineering Decision Support*, vol. 18. Springer, 2012.

[91] A. S. Sayyad and H. Ammar, "Pareto-optimal search-based software engineering (POSBSE): A literature survey," in *Proc. 2nd Int. Workshop Realizing Artif. Intell. Synergies Softw. Eng. (RAISE)*, San Francisco, CA, USA, 2013, pp. 21–27.

[92] B. F. Spencer and L. A. Bergman, "On the estimation of failure probability having prescribed statistical moments of first passage time," *Probabilistic Eng. Mech.*, vol. 1, no. 3, pp. 131–135, Sep. 1986.

[93] R. V. Roy, "Asymptotic analysis of first-passage problems," *Int. J. Non-Linear Mech.*, vol. 32, no. 1, pp. 173–186, Jan. 1997.

[94] J. He and Y.-G. Zhao, "First passage times of stationary non-Gaussian structural responses," *Comput. Struct.*, vol. 85, nos. 7–8, pp. 431–436, Apr. 2007.

[95] K. Schittkowski, "NLPQL: A FORTRAN subroutine solving constrained nonlinear programming problems," *Ann. Oper. Res.*, vol. 5, no. 2, pp. 485–500, 1986.

[96] D. C. Liu and J. Nocedal, "On the limited memory BFGS method for large scale optimization," *Math. Program.*, vol. 45, nos. 1–3, pp. 503–528, Aug. 1989.

[97] X. Xu, W. Zhao, C. Wang, and W. Chen, "Parameters optimization of differential assisted steering for electric vehicle with motorized wheels based on NLPQL algorithm," *J. Central South Univ. (Sci. Technol.)*, vol. 43, pp. 3431–3436, 2012.

[98] S. K. Mishra, P. Ganapati, S. Meher, and R. Majhi, "A fast multiobjective evolutionary algorithm for finding wellspread Pareto-optimal solutions," KanGAL, Indian Inst. Technol., Kanpur, India, Tech. Rep. 2003002, 2002.

[99] P. K. Shukla and K. Deb, "On finding multiple Pareto-optimal solutions using classical and evolutionary generating methods," *Eur. J. Oper. Res.*, vol. 181, no. 3, pp. 1630–1652, Sep. 2007.

[100] T. Homem-de-Mello and G. Bayraksan, "Monte Carlo sampling-based methods for stochastic optimization," *Surv. Oper. Res. Manage. Sci.*, vol. 19, no. 1, pp. 56–85, Jan. 2014.

[101] K. Breitung and M. Hohenbichler, "Asymptotic approximations for multivariate integrals with an application to multinormal probabilities," *J. Multivariate Anal.*, vol. 30, no. 1, pp. 80–97, Jul. 1989.

[102] S. M. Savaresi, M. Tanelli, and C. Cantoni, "Mixed slip-deceleration control in automotive braking systems," *J. Dyn. Syst., Meas., Control*, vol. 129, no. 1, pp. 20–31, Jul. 2006.

[103] C. A. Mattson and A. Messac, "A non-deterministic approach to concept selection using s-Pareto frontiers," in *Proc. Int. Design Eng. Tech. Conf. Comput. Inf. Eng. Conf. (ASME)*, 2002, pp. 859–870.

[104] C. Bucher and T. Most, "A comparison of approximate response functions in structural reliability analysis," *Probabilistic Eng. Mech.*, vol. 23, nos. 2–3, pp. 154–163, Apr. 2008.

[105] C. Proppe, "Estimation of failure probabilities by local approximation of the limit state function," *Struct. Saf.*, vol. 30, no. 4, pp. 277–290, Jul. 2008.

[106] X. Zhou, K. Li, Z. Yang, G. Xiao, and K. Li, "Progressive approaches for Pareto optimal groups computation," *IEEE Trans. Knowl. Data Eng.*, vol. 31, no. 3, pp. 521–534, Mar. 2019.

[107] H. Ren, J. Cheng, and A. Huang, "The complex variable interpolating moving least-squares method," *Appl. Math. Comput.*, vol. 219, no. 4, pp. 1724–1736, Nov. 2012.
[108] P. Ngatchou, A. Zarei, and A. El-Sharkawi, "Pareto multi objective optimization," in *Proc. 13th Int. Conf. Intell. Syst. Appl. Power Syst.*, 2005, pp. 84–91.
[109] Z. Wang and G. P. Rangaiah, "Application and analysis of methods for selecting an optimal solution from the Pareto-optimal front obtained by multiobjective optimization," *Ind. Eng. Chem. Res.*, vol. 56, no. 2, pp. 560–574, Jan. 2017.
[110] M. Liu and D. M. Frangopol, "Bridge annual maintenance prioritization under uncertainty by multiobjective combinatorial optimization," *Comput.-Aided Civil Infrastruct. Eng.*, vol. 20, no. 5, pp. 343–353, Sep. 2005.
[111] H. Furuta and T. Kameda, "Application of multi-objective genetic algorithm to bridge maintenance," in *Proc. IFIP Conf. Syst. Modeling Optim.*, 2005, pp. 139–148.
[112] B. Li, H. Du, and W. Li, "Comparative study of vehicle tyre–road friction coefficient estimation with a novel cost-effective method," *Vehicle Syst. Dyn.*, vol. 52, no. 8, pp. 1066–1098, Aug. 2014.
[113] A. Ružinskas and H. Sivilevičius, "Magic formula tyre model application for a tyre-ice interaction," *Procedia Eng.*, vol. 187, pp. 335–341, Jan. 2017.

AMINREZA KARAMOOZIAN received the B.Sc. and M.Sc. (Hons.) degrees in mechanical engineering from the Amirkabir University of Technology (Tehran Polytechnic), Iran, and the Ph.D. degree in mechanical engineering from the Nanjing University of Science and Technology, Nanjing, China. He joined the School of Automotive and Traffic Engineering, Jiangsu University, in 2019. His research interests include stability and dynamic analysis of microstructures and cellular structures, specially lattices, vehicle dynamics, advanced driver assistance systems (ADAS) for active safety applications, and reliability analysis of mechanical systems.

HAOBIN JIANG was born in Jiangsu, China, in 1969. He received the B.S. degree in agricultural mechanisation from Nanjing Agricultural University, Nanjing, China, in 1991, and the M.S. and Ph.D. degrees in vehicle engineering from Jiangsu University, Zhenjiang, China, in 1994 and 2000, respectively. His research interests include vehicle dynamic performance analysis and electrical control technology.

CHIN AN TAN received the B.Sc. degree in mechanical engineering from UC Berkeley, the M.S. degree in aeronautics from the California Institute of Technology (Caltech), and the Ph.D. degree in mechanical engineering from UC Berkeley. He is currently a Professor of mechanical engineering with Wayne State University. His research skills and interests include structural dynamics, vibration, and control, systems analysis, and mechatronics. He has many years of experience working on research problems with applications to automotive engineering (disc brake dynamics and advanced manufacturing). He is a Fellow of the American Society of Mechanical Engineers. He was the Associate Dean for Academic Affairs in the College.